Seasonal Sinking rates of Transparent Exopolymer Particles (TEP) concentrations with associated Carbon flux in adjacent Bohai Sea and Yellow Sea

M Shahanul Islam[1,2,3], Sun Jun[2,3*], Li Xiaoqian[2,3], Leng Xiaoyun[2,3]

1. College of Food Engineering and Biotechnology, Tianjin University of Science and Technology University, Tianjin 300457, China
2. Tianjin Key Laboratory of Marine Resources and Chemistry, Tianjin University of Science and Technology, Tianjin 300457, PR China
3. Research Centre for Indian Ocean Ecosystem, Tianjin University of Science and Technology, Tianjin 300457, China

*Corresponding Author: phytoplankton@163.com

Abstract

Experiments on seasonal distributions and sedimentation of transparent exopolymer particles (TEP) and its impacts on carbon cycle were carried out at three different depths in the Bohai Sea (BS), North Yellow Sea (NYS) and South Yellow Sea (SYS). Total 56 stations were sampled for TEP and its sinking rate by SETCOL method during autumn (2014), summer (2015) and winter (2015). Temperature, phytoplankton, chlorophyll-*a* (Chl-*a*) and salinity with five nutrients, phosphate (DIP), silicate (DSi), dissolved inorganic nitrate (DIN) (including nitrite, nitrate and ammonium) samples were also collected and measured for correlation analysis to visualize the seasonal effects on TEP concentrations and its sinking. Average of total TEP (2.13±0.95 μg Xeq L^{-1}) was higher in NYS (3.32±1.5 μg Xeq L^{-1}) costal currents with highest average TEP during winter (6.17 μg Xeq L^{-1}) specially in NYS (7.00±6.20 μg Xeq L^{-1}) through coastal current mixing zone. Average of total sinking rates (1.03 mD^{-1}) was higher in SYS (1.09 mD^{-1}) through mid-water layer than other seas, especially in autumn (1.13 mD^{-1}) with higher seasonal average sinking rates at summer (1.04 mD^{-1}). Carbon associated with TEP (TEP-C) was averagely distributed (1.47 μg C L^{-1}) at subsurface layer of study areas. Seasonal highest distribution of TEP-C was 4.44 μg C L^{-1} during winter, mostly in NYS. Dominant phytoplankton species *Paralia sulcata, Thalassisira excentrica* and *Rhizosolenia styliformis* maintained average correspondences with TEP which may indicate the influences of them on TEP concentration. Coastal stations were averagely clustered together in multivariate analysis after congregating oceanic stations in other groups. Species based relations were generated by Pearson correlation analysis. CCA revealed that

average close correspondence of TEP with Chl-*a* during autumn and with nutrient during winter.

Keywords: Transparent Exopolymer Particles, sinking rate, carbon sink, seasonal variation, Bohai Sea, Yellow Sea.

1 Introduction

Transparent exopolymer particles (TEP) are macro-gels like substances that play an active role between the particulate and dissolved organic carbon pools (POC and DOC, accordingly), by extending the size continuum, in addition to assisting particle formation in the marine carbon cycle (Alldredge et al., 1993; Passow, 2002b; Verdugo et al., 2004). TEP are generally considered as transparent particles which can be stainable by Alcian Blue, a dye that favorably binds to acidic polysaccharides after complexing with carboxyl groups and sulfate (Alldredge et al., 1993; Passow and Alldredge, 1995). Abiotically TEP produced from dissolved polysaccharide secretion by phytoplankton (Logan et al., 1995; Passow, 2002b; Thuy et al., 2015). As TEP possess surface-active characteristics with neutral buoyancy, they are scavenged easily with gas bubbles (Wurl et al., 2011a; Wurl and Holmes, 2008) and aggregated at the sea surface layer which can make organic sea surface microlayer (SML) accordingly (Azetsu-Scott and Passow, 2004; Cunliffe et al., 2013; Mopper et al., 1995; Wurl et al., 2009) to contribute in the increment of sea spray aerosols produced from film droplets (Aller et al., 2005).

A combined effect of regional biological and physical factors, including salinity, air-driven turbulence and production of dissolved polysaccharide primer by phytoplankton and bacteria can control the formation and distribution of TEP. Fluctuations of Nutrients availability can control phytoplankton community which is one of the relative factors that thrust the partitioning of organic matter between particulate and dissolved phases (Carlson et al., 1998; Conan et al., 2007; Lomas and Bates, 2004; Thornton, 2014). It also influences the source of organic matter and production of TEP (Claquin et al., 2008; Corzo et al., 2000; Mari et al., 2005; Passow, 2002a). Relationships between TEP and chlorophyll *a* (Chl-a) develop during a bloom, resembles the production of TEP by phytoplankton (Passow, 2002b). This relationship during bloom phase is species-specific, with the cellular aggregation rate of TEP by phytoplankton caused by their growth period. So, relation patterns of TEP and chl-*a* will not match due to the variations in phytoplankton compositions with different life stages. Low nutrient increases TEP abundances through preventing TEP

consumption by bacteria (Bar-Zeev and Rahav, 2015), so that aggregation and accumulation of TEP at the sea surface as N-poor C-rich organic material (Passow, 2002b, Mari et al., 2017).

TEP are more adherer than non-TEP substances which may help in particles and subsequently increase sedimentation (Logan et al., 1995; Passow et al., 1994). As microbial hotspots, TEP and POC serve a source of carbon to the deep ocean by sinking in the water column (Jokulsdottir and Archer, 2016; Prairie et al., 2015). Although sinking process of marine aggregates have been observed (Burd and Jackson, 2009; Iversen and Robert, 2015), there remains the necessity of understanding about the effect of TEP in the biological carbon pump (Burd et al., 2016; Zetsche and Ploug, 2015). TEP sinking rate measurement experiments in Changjinag (Yangtze River) estuary near East China Sea during summer showed higher sedimentation of TEP at the upper water column than deep seas (Guo & Sun 2018). It also showed the higher sinking rat of TEP in the summer rather than spring which may have important role on carbon exports in that area.

The present study was conducted through the semi-closed Bohai Sea (BS) and Yellow Sea which covered a big part of the north Chinese seas. Semi enclosed BS is located at the north-eastern continental region of China (Xu et al. 2010). With sensitive primary productivity and commercial fishery (Tang et al. 2003, Huang et al. 1999), BS got waste water-loads and inputs from the Tianjin City as well as Liaoning, Shandong and Hebei provinces (Xu et al. 2010). There is another semi-enclosed marginal sea of the western Pacific Ocean at the southern-east of BS, called Yellow Sea (Liu et al. 2015b). Yellow Sea possesses various oceanic processes through seasons (Hwang et al. 2014; Su 1998; Yuan et al. 2008; Isobe 2008). Zonation of Yellow Sea i.e. North Yellow Sea (NYS) and South Yellow Sea (SYS); will help in visualization of better seasonal scenario (Li et al. 2017). In autumn, appurtenance of Yellow Sea cold water mass (YSCW) at SYS influenced the vertical mixing of NYS water (Zou et al. 1999). The Yellow Sea Warm Current (YSWC) acted at SYS during winter (Gao et al., 2004, Su 1998) and Changjiang Diluted water (CDW) during summer (Naimie et al. 2001). Fishery (Tang and Su, 2001), biological community (Hyun and Kim, 2003; Fu et al., 2009; Zhang et al., 2009) and ecological problems raises the importance of researches on Yellow Sea (Sun et al., 2011; Tang et al., 2007, 2010).

Studies on TEP and its sinking rates showed correlation with environmental parameters i.e. temperature (Claquin et al. 2008, Fukao et al. 2012), salinity (Mari et al.

2012), microbial breakdown (Mari et al. 2017) and phytoplankton species composition (Passow 2002b). Changes in TEP assemblage may also influenced by bacterial secretions and feeding as well as zooplankton grazing locally (Passow and Alldredge, 1999, Surosz et al. 2006, Mari et al. 2017). It also showed correlation with nutrients in different studies (Corzo et al. 2000, Mari et al 2005). Seasonal variation of parameters can be a cause behind these phenomena. Poor correlations among TEP and these environmental parameters can be found due to limited data and insignificant variations in salinity and nutrients from sampling stations (Guo & Sun 2018). Seasonal distribution and sinking rate of TEP will describe more specific relation of TEP with other environmental parameters. On the basis of these objectives, present study was conducted on sinking flux of TEP and its concentration with related carbon exports through three separate seasons (autumn, summer, winter) in the Bohai and Yellow Sea of China from 2014-2015.

2 Materials and Methods

2.1 Study area and sample collection

Water sample (1 liter) was taken from three different depths (0-100 meters) at various stations (Fig. 1) during 2014-2015 in Bohai Sea (BS), North Yellow Sea (NYS) and South Yellow Sea (SYS). Session for autumn sampling was conducted between 8-22 November (Fig. 1A), 2014, summer sampling from 18 August to 22 September, 2015 (Fig. 1B) and winter sampling in Bohai Sea and North Yellow Sea from 17 October to 22 November, 2015 (Fig. 1C). Boundary currents flow directions in Bohai Sea and Yellow Sea were changed with seasons (Fig. 2). Korean coastal currents (KCC) flows northward in summer and southward in winter. YSWC was found during winter and CDW flows eastward during summer. Remain costal currents and warm currents flows in their constant direction (Hwang et al. 2014; Su 1998; Yuan et al. 2008; Isobe 2008) which may have distributary effect on these particles concentration and its sinking rates besides all hydrological parameters.

Sample collection was done by multiple rosette (with CTD sensors) for different depths at each sampler stations based on bottom depth. Each station wat designed with three distinguishing depths for better graphical analysis. Samples were collected seperately to determine phytoplankton composition, chl-*a* concentration, nutrients, TEP abundances and its sinking rates. Due to shallow water, depths were limited in each station between 0-100 meters. In 1L sampling bottles, phytoplankton samples were collected with 1% formaldehyde concentration for further analysis (Guo and Sun 2018). Sea water were collected in 100 mL

sample bottle from all sampling depths and stored at -25^{o}C for nutrient analysis of each station. CTD sensors recorded temperature and salinity was determined while sampling from different depths from study area.

2.2 Biological parameters

According to Welschmeyer (1994), chlorophyll – a (chl a) were measured after filtering seawaters from all stations by 25 mm GF/F filters (Whatman^{TM}) and then reserved at -20°C in the dark until analysis (less than 35 days). 90% acetone were used for extraction of chl-a for 24 h at -20°C in the dark, and samples were then analyzed by a laboratory fluorometer called Turner-Designs Trilogy^{TM}. Phytoplankton sample (1 Liter, preserved with 1% formaldehyde) were analyzed according to modified Utermöhl methods followed by Sun et al. (2002) after arranging the samples (25 mL) in Utermöhl counting chamber (being settled for 24 hrs.) in inverted microscope. Dominance index was used to describe phytoplankton dominant species under this equation:

$$Y = \frac{n_i}{\mathbf{N}} \times f_i$$

Where, N is the total cell abundance of all species, n_i is total cell of species *i* and f_i is the count of occurrence of species *i* in all sample (Guo et al. 2014).

2.3 Chemical analysis

Nutrients i.e. dissolved inorganic phosphate (DIP), dissolved inorganic nitrogen (DIN), dissolved silicates (DSi), ammonium, nitrate & nitrite analysis were measured by fully automated (SANPLUS, Dutch SKALAR company) wet chemical analyzer (Liu et al., 2015a). Sextuplicate measurements of TEP were done by following colorimetric method of Passow and Alldredge (1995) for all samples after confirming calibration factor (f_x) from xanthan gum curve. At least 50 mL (V_f) sample sea water were thoroughly filtered (4-6 replicates) at low and fixed vacuum (150 mm of Hg) through polycarbonate filters (0.4-pm pore-size) and dye binding particles on the filter for approximate 2 seconds with 500 micro liters of 0.02% alcian blue (8GX; aqueous solution) in 0.06% acetic acid (pH 2.5). After staining, filters are rinsed carefully with distilled water to prevent excess dye once. Dye bound to substrates will not wash off by this rinsing. Then filters were soaked into 25 mL beakers with 6 mL of 80% sulfuric acid and kept for 2 hours. The beakers were gently shacked for 3-5 times during soaking period. Maximum absorption of the solution (E_{787}) lied at 787 nm and it was

158 measured (μg Xeq. L^{-1}) in a l cm cuvette (B_{787}) against distilled water as a reference. The
159 equation is:

160 $$TEP = (E_{787}\text{-}B_{787}) \times (V_f)^{-1} \times fx$$

161 Where, fx = Average calibration factor and it was 9.83 μg from the graph of xanthan
162 gum curve. Calculation of TEP-carbon (TEP-C, μg C L^{-1}) was determined with the slope
163 (0.75) from the equation as follows (Engel &Passow 2001):

164 $$TEP\text{-}C = 0.75 \times TEP_{color}$$ (Guo & Sun 2018)

165 where TEP_{color} is the TEP concentration (TEP) with the unit of μg Xeq L^{-1}.

166 **2.4 Measurement of TEP sinking flux**

167 TEP sinking rates were determined at each station, and the SETCOL method was used
168 to measure the sinking rates on research vessel according to Bienfang (1981). For
169 measurements, a Plexiglass column (height = 0.45 m and volume = 750 mL) was filled
170 completely with a homogeneous water sample within 10 min after sampling, and a cover was
171 then placed on the set-up. The Plexiglass columns were kept undisturbed on the vessel to
172 settle for 2-3 hours. Temperature was maintained through a thermostatically controlled water
173 bath with water jackets by pumping its water. The settled sample of experiment was collected
174 in sample bottles by successively draining the upper, middle, and bottom compartments of
175 the Plexiglass column via piped outlet in the wall of column. The TEP biomass was measured
176 after the settlement in the samples from all three compartments. These measurements were
177 combined to calculate the sinking rate of TEPs according to the formula:

178 $$TEP_s = \frac{B_s}{B_t} \times \frac{L}{t}$$

179 where V = sinking rate; B_s = the biomass of TEP settled into the bottom compartment; B_t =
180 the total biomass of TEPs in the column; L = length of the column; and t = settling interval.
181 Samples from all depts were triplicated during measurement for better data analysis and
182 marked according to stations about sinking rate as well as TEP concentrations.

183 **2.5 Data analysis**

184 Analysis and discussions were forwarded with seasonal (autumn, summer & winter) and
185 oceanic (Bohai Sea, North Yellow Sea & South Yellow Sea) categories accordingly (Table
186 1). Various multivariate analyses were performed by using Multi Biplots software (Vicente

Villardón, 2015) on recorded data. Single cluster analysis was performed by Multivariate Statistical Package Software with Baroni-UrbaniBuser Coefficient. Linear regression, Pearson correlation and covariance were performed by Microsoft Excel 2016 software. Canonical correspondence analysis (CCA) were done by Canoco software, version 4.14 (CANOCO for Windows; Ter Braak & Šmilauer, 2002). For integrated surface view of recorded and examined parameters during winter 2015, Surfer 12 was used. Box-whisker plots by Microsoft Excel 2016 showed the range of recorded TEP and TEP_s through different water layers after stations' integration. Concentrations of different parameters were graphically presented by Ocean Data View (ODV 2016) software.

3 Results

3.1 Environmental Hydrology

Study stations were segmented on the basis of sea for better understanding about present observtions during autumn 2014 (Fig. 1A), summer 2015 (Fig. 1b) and winter 2015 (Fig. 1C). Sampling stations (St.s) of autumn through the Bohai Sea (St.s B45 - B68), North Yellow Sea (St.s B04 - B34) and South Yellow Sea (St.s H07 - H40) were determined by geographical positions (Fig. 1D). Similarly, the stations of Bohai Sea (St.s B45 - B68), North Yellow Sea (St.s B04 - B34) and South Yellow Sea (St.s H07 - H38) were associated accordingly in summer. In winter, sampling was done only in Bohai Sea (St.s B42 - B68, BS1 & BS5) and North Yellow Sea (St.s B04 - B33), except SYS.

The Bohai Sea and Yellow Sea had a complex dynamic environment with various seasonal and local geophysical currents (**Fig**. 2). Seasonal currents flow maps (Fig. 2) were drawn on the basis of secondary data and previous literatures (Hwang et al. 2014; Su 1998; Yuan et al. 2008; Isobe 2008) from that area due to track the possible water mass effect on TEP distribution. Average concentration of all parameters through every season showed high chl-*a* concentration along coastal zones of BS and NYS. Average annual TEP was higher at BS along BSCC, at NYS along YSCC and at SYS along CDW. Average annual nutrients were highly concentrated at BS than other seas, except nitrite at YSCC of SYS (Table 1). Adequate T-S diagrams noted out stations aggregations at different seasonal water masses through seas i.e. low temperature low salinity (LTLS), low temperature high salinity (LTHS), high temperature low salinity (HTLS) and high temperature high salinity (HTHS) accordingly (Fig. 3). All stations of BS were scattered at LTLS (Fig. 3A) and NYS at LTHS (Fig. 3B) during autumn due to lower sampling depth, influenced by surface mixing. SYS

were segmented into HTHS and LTHS in both autumn (Fig. 3C) and summer (Fig. 3F); followed by NYS in summer only (Fig. 3E). Due to high surface temperature, stations with lower depths of BS were assembled at HTLS (Fig. 3D). During winter, low temperature influenced the stations of BS and NYS to LTHS zone (Fig. 3G).

3.1.1 Vertical concentrations in autumn 2014

During autumn (Fig. 4A), TEP was higher at the north of NYS along LCC and CWC of southern SYS (Fig. 4D). Temperature were higher at YSCC of SYS and salinity were dense at KCC of NYS and SYS with high Chl-*a* was at LCC of NYS. Concentrations of nutrients were higher at BS except nitrite. Nitrite was higher at LCC of NYS and at YSCC of SYS. DIP. DIN, DSi and nitrate were higher at the southern part of SYS through whole autumn (Table 1). Vertical profile showed higher concentration of TEP of SYS with high temperature too, especially at St. H33, H35 and H40. Chl-a was dense in NYS (St. B15, B19 and B25) where DSi was dramatically low. Nutrients i.e. DIN, nitrate and ammonium were found higher at the bottom of BS, especially at St. B45, B49 and B57. Salinity was lower at surface of whole study area. DIP found lowest at surface stations i.e. H07 and H09 of SYS but highest at bottom of B34 and H07 stations. Nitrite was found higher at the SCM of NYS and SYS (Table 1). During autumn, dominant phytoplankton were *Paralia sulcate, Coscinodiscus* sp., *Ceratiumfusus, Thalassiosira sp., Probosica alata f. indica, Ceratiumtripos, Nitzschia* sp., *Thalassiosira pacifica, Guinardia delicatula* and *Thalassiosira excentrica* sequentially.

3.1.2 Vertical concentrations in summer 2015

Through summer (Fig. 4B), TEP was higher at southern SYS (Fig. 4E) with high temperature and nutrients (DIP, DIN, DSi and nitrates). Notably, DIP found high at CWD of SYS. In BS, nitrate and nitrite were higher at south coast and ammonium was higher at north-west coast with high temperature. Salinity was aggregated at KCC of NYS and mid SYS. Chl-*a* was dense at YSCC of NYS and CDW of SYS (Table 1). With obvious high temperature, summer possessed low TEP at surface of BS. TEP was higher with low nutrients and chl-a at the SCM of Station B45. DIN, nitrate and nitrite were high near station B68. DIP and DSi were higher at the bottom of Station B57 in BS. TEP was comparatively low at NYS with high chl-a at SCM and bottom of Station B25. DIP, DSi and nitrate were higher at the bottom of Stations B04 and B11. *Alexandrium tamarense, Rhizosolenia styliformis, Paralia sulcate, Guinardia flaccida, Dinophysis sp., Ceratium fusus, Thalassiosira excentrica,*

Ceratium furca, Dictyocha fibula and *Diploneis bombus* were dominant phytoplankton accordingly through study area in summer. In SYS, TEP was higher at the SCM with low nutrients and chl-a as BS (Fig. 4E). Nutrients along with salinity were higher at the bottom of Station H07 and H09.

3.1.3 Vertical concentrations in winter 2015

In winter (Fig. 4C), TEP was dense at KCC of NYS, especially at SCM (Fig. 4F) with high temperature and salinity. However, chl-*a* was higher at the north coast and BSCC of BS with YSCC of NYS too. Most of the nutrients were higher at BSCC of BS except DIP. DIP found higher at the transitional zone of BS and NYS.DSi concentration was also higher at KCC of NYS. During winter, NYS showed higher abundances of Chl-a and salinity at the stations (B04, B25 & BS5) near YSCC. Higher TEP was found at SCM of NYS than BS. Temperature was recorded lowest in BS than NYS (**Fig**. 1), especially near shore area. Phytoplankton i.e. *Paralia sulcate, Thalassiosira excentrica, Actinoptychus* sp., *Donkinia recta, Thalassiosira sp., Coscinodiscus* sp., *Coscinodiscus subtilis, Navicula* sp., *Pleurosigma pelagicum* and *Coscinodiscus radiatus* were dominant during winter. Nutrients i.e., DIN, DSi, ammonium, nitrate and nitrite found higher at the SCM of Bohai Sea. DIP was found abundance in surface area at the transitional area (near Station B33) of BS and NYS (Table 1). Average nutrients were higher in BS than NYS during winter 2015. Stations near coastal area of BS (B45 & B68) and NYS (B04, B25 & BS5) have higher nutrients comparatively.

3.2 Seasonal and regional TEP concentration with carbon association

Present study measured 2.13 μg Xeq. L^{-1} as average TEP concentration (TEP) which is ranged between 0.2-23.20 μg Xeq. L^{-1}. NYS (2.32 μg Xeq. L^{-1}) has more TEP concentration in average than SYS (1.18 μg Xeq. L^{-1}) and BS (2.08 μg Xeq. L^{-1}). Apparently, winter season (6.17 μg Xeq. L^{-1}) shows higher average concentration of TEP in each sea (Table 1) than in summer (1.10 μg Xeq. L^{-1}) and in autumn (0.67 μg Xeq. L^{-1}). SYS showed higher TEP in autumn (0.93 μg Xeq. L^{-1}) and in summer (1.42 μg Xeq. L^{-1}) at HTHS (Fig. 5C & 5F). In BS, assemblage of TEP was higher at LTLS during summer (Fig. 5D) than autumn (Fig. 5A). Apparently, TEP was higher at LTHS of NYS during summer (Fig. 5E) and winter (Fig. 5G) than autumn (Fig. 5B).

The carbon (TEP-C) associated with TEP picked at winter 2015 and became lower during autumn 2014. BS showed low carbon abundance at surface during summer (Fig. 6E). NYS possessed high TEP-C in SCM during winter (Fig. 6J) and at bottom during autumn and

summer (Fig. 6B & 6F). Surface of SYS recorded high TEP-C than BS and NYS during summer (Fig. 6G). However, SYS also possessed comparatively high verity of TEP-C than BS and NYS at its SCM during autumn and summer (Fig. 6D & 6H). Average TEP-C showed high variation at SCM through study areas (Fig. 6L). Average TEP-C was 1.47 μg C L^{-1} with seasonal highest 4.44 μg C L^{-1} during winter specially in NYS (5.25 μg C L^{-1}). SYS has higher TEP-C during autumn (0.58 μg C L^{-1}) and summer (1.07 μg C L^{-1}) than other seas. Highest TEP-C was found at SML of stations B15 (15.78 μg C L^{-1}), B22 (17.40 μg C L^{-1}) and B33 (10.91 μg C L^{-1}) of NYS during winter which showed close cluster during analysis (Fig. 9C; Grpup 8).

3.3 Seasonal and regional TEP sedimentation

Sedimentation or sinking rates of TEP was recorded 1.03 mD^{-1} in average of all seasons (Table 1) at study area. TEP sinking rate was higher in summer (1.04 mD^{-1}) than autumn (1.02 mD^{-1}) and winter (1.03 mD^{-1}). However, winter showed high sinking rates (1.02 mD^{-1}) in BS than its summer (1.01 mD^{-1}) and autumn (0.9 mD^{-1}) data. On the other hand, comparatively high sinking rates were measured in SYS during autumn (1.13 mD^{-1}) than its summer (1.05 mD^{-1}). SYS also possessed average high sinking rates of TEP (1.09 mD^{-1}) than BS (0.9 mD^{-1}) and NYS (1.03 mD^{-1}).

3.4 TEP sinking in segmented depths

Average TEP sinking dynamics were similarly close in average at each depth (Fig. 7K). In BS, high sedimentation variation was observed at mid layer (Fig. 7A) during autumn (0.72-1.16 mD^{-1}) and at surface (Fig. 7E, 7I) during summer (0.86-1.57 mD^{-1}) and winter (0.64-2.06 mD^{-1}). Surface of NYS (Fig. 7B) has diverse sinking rates during summer (0.77-2.47 mD^{-1}), mid layer (Fig. 7F) in winter (0.72-1.53 mD^{-1}) and bottom (Fig. 7J) in autumn (0.76-1.19 mD^{-1}). Surface of SYS (Fig. 7C) during summer (0.62-2.40 mD^{-1}) and bottom layers (Fig. 7G) during autumn (0.78-1.55 mD^{-1}) showed sedimentation variation accordingly. In average, bottom layer (Fig. 7D) during autumn (0.72-1.55 mD^{-1}) and surface of study area during summer (0.62-2.47 mD^{-1}) and winter (0.64-2.06 mD^{-1}) possessed high sinking dynamicity (Fig. 7D, 7H & 7L).

3.5 Correspondence relationships of TEP

TEP showed close correspondent relationship with DIP and chl-*a* in average (Fig. 8I) and in winter at BS (Fig. 8F) after applying CCA. However, winter at NYS showed TEP was

corelated with nitrate through each station. In autumn, TEP showed average close correspondence with nitrite in CCA across study areas (Fig. 8A, 8D, 8G & 8J). During summer, TEP was averagely compliance with nitrite (Fig. 8D) through all seas (Fig. 8H and 8I) except at BS (nitrate; Fig. 8E). In average, TEP showed close correspondences with *T. excentrica* and *P. sulcata* during autumn, *R. styliformis* in summer and *P. sulcate* and *Actinoptychus* sp. were dominant across study area. Both in BS and NYS, *P. sulcata* was highly dominant and mostly correlates with concentration of TEP through all seasons. In SYS, correspondences of dominant phytoplankton with TEP were observed rather than nutrients (Fig. 8J & 8K).

Considering all parameters, most of the SYS stations clustered closely in dendrogram (Group 1 and 4) after applying Baroni-Urbani Buser coefficient during autumn (Fig. 9A) and summer (Fig. 9B). In BS, St. B45 clustered in same group with B68 through all season (autumn; group 2, summer; Group 5 and winter; Group 7). St. B15 of NYS showed group correspondence with St. B25 during autumn (Fig. 9A; Group 2) and winter (Fig. 9C; Group 8) except summer. Rest of the stations clustered randomly with each other due to their different gradients.

4 Discussions

4.1 Seasonal effect on TEP distribution

Study of seasonal trends on EPS (exopolymeric substances i.e. TEP) confirmed the formation of EPS at earlier season in upper sea column with time (Riedel et al. 2006, Collins et al. 2008). Traditionally, phytoplankton cells were reported as precursors of TEP, especially under bloom situations (Hong et al. 1997; Passow 2002a; Passow and Alldredge 1994). Moreover, Changes in TEP influenced by a balance between sources i.e. production by algae, bacteria, and possibly other organisms (Ortega-Retuerta et al. 2010). In BS, *Skeletonema costatum* and *Coscinodiscus oculus-iridis* during winter and *Noctiluca scintillans, Chaetoceros affinis, Chaetoceros* sp. through all seasons were reported as dominant phytoplankton species (Yang et al. 2018) which may have local influence on TEP (Passow 2002a). However, *P. sulcata* showed dominancy in BS through 3 seasons BS by corresponding closely with TEP (Fig. 8D, 8E & 8F). During autumn at NYS, *Pseudo-nitzschia pungens* and *Proboscia alata* were reported dominant at the same location of dense TEP compared to present study (Li et al. 2017) which may also liable for TEP assemblages by demonstration close relation in CCA (Fig. 8G). In SYS, dominancy of *Paralia sulcate* and

Thalassiosira angulate (Li et al. 2017, Liu et al. 2015a) with *Pseudo-nitzschia pungen* (Li et al. 2017) were reported at same magnitudes during autumn which were similar to present study and also maintained close correspondences with TEP (Fig. 8J). Coastal SYS showed the dominancy of *Skeletonema costatum* and *Thalassiosira nordenskiodii* during winter (Wen et al. 2007). Among phytoplankton, cyanobacteria (36%) were reported stratified during summer at SYS (Liu et al. 2015b). Phytoplankton i.e. *Paralia sulcata*, *Prorocentrum dentatum* and *Thalassiosira angulata* were abundant species at south of SYS which area were highly concentrated with TEP (**Fig. 6**A) according to present study. Biological process of these species may liable for the abundance of TEP along with those study areas.

However, TEP can be high in lower biological activity (Mari et al. 207). In absence of phytoplankton, dissolve organic matter can be source of TEP (Wurl et al. 2011b). During autumn and summer, TEP was abundant with high nutrients and low Chl-*a*. Arctic autumn showed low TEP concentrations in upper water layer with no significant enrichment (Wurl et al. 2011). Though, limited sampling data showed no significant correlation of TEP with nutrients and salinity in Changjinag (Yangtze River) estuary (CE) near East China Sea (Guo & Sun 2018). However, TEP was higher along CDW from CE during this study at summer. Consumption by various organisms (Tranvik et al. 1993) can also change TEP distribution. In some places, organisms may feed on TEPs due to low nutrient concentration which is why TEP is very low in those areas during summer and autumn (**Fig**. 4). Higher tempered zone also possessed high TEP production due to the effect of temperature on photosynthetic parameters (Claquin et al. 2008, Fukao et al. 2012) which supported high TEP assemblage at HTLS through BS during summer (Fig. 5D) and at HTHS of SYS during summer and Autumn (Fig. 5C & 5F). It also influenced high TEP concentrations in various estuaries and seas during summer and spring than other seasons (Table 4). Semi enclosed Aegean Sea was reported with increased TEP during summer than autumn due to phytoplankton production and bacterial activity (Parinos et al. 2017). Similar seasonal TEP pattern was observed at semi embedded BS (Table 1) which also possessed close correspondences with dominant *P. sulcate* (Fig. 8E).

During summer, TEP was high at CDW generating Changjinag (Yangtze River) estuary near East China Sea than spring due to high primary productivity (Table 4; Guo & Sun 2018). Similarly, TEP was also found higher near CDW cruising area of SYS during summer (Fig. 4B) with high chl-*a* than others seas (Table 1). Arctic winter season also showed the highest TEP concentrations and formation rates until spring due to algal activity

(Wurl et al. 2011b) which interprets prior TEP concentration during winter than other seasons with high chl-*a* along study areas (Table 1). Species' closer correspondences with TEP during winter (Fig. 8C) and summer of SYS (Fig. 8K) also supported these statements. Notably, Oligotrophic reservoir was also reported with high TEP during summer than other seasons (Vicente et al. 2009).

Studies showed that mostly estuaries possessed higher average TEP at 0-50 m than bays and open seas due to higher primary productivity (Table 2). However, literatures demonstrated that highest TEP was found at the surface water column in Adriatic Sea (Radic et al. 2005) and lowest in Weddell Sea (Ortega-Retuerta et al. 2009). Average TEP was higher in western subarctic part (Ramaiah et al. 2005) than eastern (Wurl et al. 2011b) and western tropical parts (Kodama et al. 2014) as well as eastern subarctic zone (Wurl et al. 2011b) at ocean (Table 2). Higher estuarine TEP was found in Changjinag River Estuary (Guo & Sun 2018) during both in summer and spring rather than that of Jiulong River estuary (Peng and Huang 2007) and Pearl River estuary (Sun et al. 2010). Upper water column observed lower average TEP at LTLS of BS than in Chesapeake Bay (Malpezzi et al. 2013) and Gulf of Cadiz (Garc et al. 2002). However, surface water column of North Pacific Ocean possessed higher TEP than below 50 meters due to high biological production (Table 3). Consequently, average seasonal TEP concentration was found higher at surface water column of study area (Fig. 4).

Similarly, deep water column of bays was reported with high TEP concentration than seas and open oceans due to higher primary production (Table 3). Gulf of Aqaba showed highest TEP below 50 meters of any seas (Bar-Zeev et al. 2009). Deep water column of Aegean sea was reported with high TEP during autumn (Parinos et al. 2017) which is similar to SYS (St.s H35 & H40; Fig. 4D) through same season. Below 100m, TEP was higher in Eastern Mediterranean Sea (Bar-Zeev et al. 2011) than other part of this sea (Ortega-Retuerta et al. 2010) and Gulf of Aqaba (Bar-Zeev et al. 2009). Average vertical TEP profiling was higher in Ross Sea (Hong et al. 1997) than rest seas (Table 2). Bacterial activity and phytoplankton excretions were liable for these dispersion (Parinos et al. 2017, Mari et al. 2017). Average TEP was observed high at LTHS (Fig. 3G) in Bohai Sea (Fig. 5C) through BSCC (Fig. 2C) during winter (Fig. 4C) with highest chl-*a* (Table 1). High productivity may initiate these phenomenon (Wetz et al. 2009). However, LTHS of NYS showed high TEP during winter (Fig. 5G) than other seasons (Fig. 5B & 5F). On the other hand, SYS picked

high TEP at HTHS during autumn (Fig. 5C) than rest seasons (Fig. 5F). Combined effects of seasonal environmental parameters may cause these variations through those water columns.

4.2 Seasonal sinking rate variations of TEP

Sinking rates or particle sedimentation of TEP can also cause changes in TEP distribution (Passow et al. 2001). SETCOL method was most popular scientific method to track it due to its simplicity and reliability (Guo & Sun 2018). However, motion and turbulence of seawater was ignored in SETCOL which have complex effect on particle sinking in ocean (Javier et al. 1996, Ruiz et al. 2004). So, the actual situation remained unclear with theories (Guo & Sun 2018). Seawater is denser than TEP (density 0.70-0.84 g cm^{-3}) which indicated that pure TEP will ascend upward in ballast free condition (Azetsu-Scott and Passow 2004). So, sinking rates of TEP can be negative (Azetsu-Scott and Passow 2004, Mari 2008). In real scenario, presence of organic and inorganic matter in seawater make complex situation for TEP to be pure. Sticky gel characteristics of TEP (Engel 2000, Rochelle-Newall et al. 2010) may aggregated them with various detritus, particles and organisms i.e. bacteria, phytoplankton and mineral clays (Prieto et al. 2002) which may influence them to sink downward in water (Mari et al. 2017).

Freshwater lake has lower particle concentration with higher sinking rates of TEP (Table 7) due to the influence of phytoplankton cells aggregation (Vicente et al. 2009). Estuarine TEP sedimentation rate was reported lower in spring than other seasons (Guo & Sun 2018). Through seas, Average sinking rate of TEP in NYS (Table 5) was observed higher in summer and winter during present study may be due to higher salinity (Table 1) and primary productivity (Chl-a). Oligotrophic reservoir was also reported with high sinking rates during late winter and early spring (Vicente et al. 2009). In SYS, highest TEP sedimentation was at Station H38 (2.40 mD^{-1}) may be caused by counter effect of CDW and CWC (Fig. 2). SYS also has higher sinking rates of TEP in autumn than BS and NYS may be due to high nutrient concentrations (Fig. 6) at the bottom that may stick with TEP to sink downwards. Rather than other coastal water (Changjiang Estuary), Bohai Sea possessed higher sinking rates of TEP in average, especially during summer (Table 5). However, open ocean was observed with low sinking rate due to is unproductive winter stratification (Mari et al. 2008). Seasonal effect on concentrations of environmental parameters and coastal currents' activity may cause these differences in sedimentation rates of TEP in study areas.

4.3 Potential role of seasonal carbon export associated with TEP

Organic carbon formations at sea surface through TEP aggregations and its sedimentation, were a complex part of the carbon cycle in ocean besides the influences of besides phytoplankton cells and zooplankton fecal pellets (Turner 2002, Turner 2015, Mari et al. 2017). These exopolymer particles contained carbon complex which may disappeared due to TEP sedimentation and degradation by bacteria (Prieto et al. 2006) in the euphotic zone. Due to alignment of TEP as same magnitude of phytoplankton cells abundance (Passow 2002b, Passow et al. 2001), TEP sinking was accepted as important carbon pathway for its dominant effect on TEP-C (Stoderegger and Herndl 1999, Obernosterer and Herndl 1995, Guo & Sun 2018). Understanding TEP-C formations and its contributions along study areas, a conceptual model of TEP was drawn on the basis of TEP assemblage and its correlations with phytoplankton concentration (Fig. 10). Bacterial production and algal activity influenced the TEP assemblage at upper water column, was shown in this 3D model (Ortega-Retuerta et al. 2010, Bar-Zeev et al. 2011). Influential arrows were drawn on these literatures. CDW influences phytoplankton dominance with high concentrations at nearby ecological provinces (Li et al. 2017, Guo et al. 2014) which may influence TEP formations at southern part of SYS. TEP-C was lower in spring than in summer at Changjiang River (Yangtze River) estuary near East China Sea.

Present study observed higher total average of TEP-C in NYS than BS and SYS especially in winter and lowest TEP-C in autumn in BS during all three seasons. Lower sinking rate can increase TEP aggregation at surface area (Stoderegger and Herndl 1999, Obernosterer and Herndl 1995, Guo & sun 2018) which may influence TEP-C at NYS. Considering the complex effect of all environmental parameters, TEP-C distribution showed similar correlations with nutrients and Chl-a as TEP in different seasons accordingly. Results of present study suggest the importance of TEP in carbon cycle in Bohai Sea and Yellow Sea. TEP controlled the biological carbon pump of atmospheric CO_2 (Mari et al. 2017). With significant seasonal TEP-C distribution and TEP correlations with phytoplankton, the data showed an unavoidable importance of TEP and its sedimentation rates for exporting carbon in study areas. Stickiness of TEP and its balances between production and degradation rates contributed in POC cycling (Mari et al. 2017) in the ocean. TEP sedimentation roughly contributes 30% in POC flux at Santa Barbara Channel (Passow et al. 2001) and 0.02%-31% in oligotrophic reservoir of southern Spain (Mari et al. 2017). POC was not measured during present study. Reports showed that TEP contributes significantly in POC (Ortega-Retuerta et

al. 2019). Further research may introduce from these limitations by measuring POC for stablishing significant correlations with TEP to contribute in local carbon cycle.

5 Conclusions

Seasonal variations of TEP concentration was complex and mostly depends on nutrients and Chl-a. Correlations on the basis of 168 samples of TEP with same amount of other environmental parameters showed variations among seas as well as seasons. Temperature varied from 0-28 ^{o}C round the year but TEP stacked from 0 to below 10 μg Xeq. L^{-1} in average. Biological productivity may liable for TEP distribution during autumn and summer, especially in SYS and nutrients for TEP in winter in BS. Coastal current mixing has an influence on TEP due to its dominancy at dilution zones. Sinking rates of TEP mostly varied at surface of BS and NYS during summer and winter. SYS has moderated sinking rates of TEP at its surface and bottom with higher nutrients concentrations. With close correspondences, dominant phytoplankton i.e. *P. sulcata*, *T. excentrica* and *R. styliformis* have influences of high TEP concentration. Average carbon exports maintained same magnitudes with TEP during each season. Average TEP sinking was diverse at SCM but higher at surface through all seasons. Further research on POC cycle by measuring TEP, TEP-C and its sinking rates with seawater density and turbidity of selected study area are recommended to be more precise on carbon contributions of exopolymers in the process of biological and chemical carbon pump in open and coastal seas.

Acknowledgements

This study was supported by National Natural Science Foundation of China (Nos. 41876134, 41676112 and 41276124), the Key Project of Natural Science Foundation for Tianjin (No. 17JCZDJC40000), the University Innovation Team Training Program for Tianjin (TD12-5003) and the Tianjin 131 Innovation Team Program (20180314), and the Changjiang Scholar Program of Chinese Ministry of Education to Jun Sun. The authors are grateful to Prof. Houjie Wang for providing the data of temperature and salinity, and also thank the crew and captain of the R/V Dongfanghong 2 for their assistance in sample collection during the cruise supported by National Natural Science Foundation of China (Nos. NORC2014 and NORC2015).

References

505 Alldredge, A.L., Passow, U., and Logan, B.E.: The abundance and significance of a class
506 of large, transparent organic particles in the ocean. Deep-Sea Res. I Oceanogr.
507 Res. Pap. 40. http://dx.doi.org/10.1016/0967-0637(93)90129-Q, 1993.

508 Aller, J.Y., Kuznetsova, M.R., Jahns, C.J., and Kemp, P.F.:The sea surface microlayer as
509 a source of viral and bacterial enrichment in marine aerosols. J. Aerosol Sci.
510 36: 801–812. http://dx.doi.org/10.1016/j.jaerosci.2004.10.012, 2005.

511 Azetsu-Scott K. : Ascending marine particles : significance of transparent exopolymer
512 particles (TEP) in the upper ocean[J].Limnology and Oceanography, 49（3
513 ） : 741-748, 2004.

514 Azetsu-Scott, K., and Passow, U. :Ascending marine particles: significance of transparent
515 exopolymer particles (TEP) in the upper ocean. Limnol. Oceanogr. 49:741–
516 748. http://dx.doi.org/10.4319/lo.2004.49.3.0741, 2004.

517 Bar-Zeev, E., and Rahav, E.: Microbial metabolism of transparent exopolymer particles
518 during the summer months along a eutrophic estuary system. Front. Microbiol.
519 6: 403. http://dx.doi.org/10.3389/fmicb.2015.00403, 2015.

520 Bar-Zeev, E.; Berman-Frank, I.; Stambler, N.; Vazquez´ Domínguez, E.; Zohary, T.;
521 Capuzzo, E.; Meeder, E.; Suggett, D.; Iluz, D.; Dishon, G.; et al. Transparent
522 exopolymer particles (TEP) link phytoplankton and bacterial production in the
523 Gulf of Aqaba. Aquat. Microb. Ecol. 56, 217−225, 2009.

524 Bar-Zeev, E., Berman, T., Rahav, E., Dishon, G., Herut, B., Kress, N., and Berman-
525 Frank, I., : Transparent exopolymer particle (TEP) dynamics in the eastern
526 Mediterranean Sea. Mar Ecol Prog Ser 431: 107−118, 2011.

527 Bienfang, P.K.: SETCOL－ a technologically simple and reliable method for measuring
528 phytoplankton sinking rates. Canadian Journal of Fisheries and Aquatic
529 Sciences.38(10): 1289-1294. https://doi.org/10.1139/f81-173, 1981.

530 Burd, A., Buchan, A., Church, M.J., Landry, M.R., McDonnell, A.M.P., Passow, U.,
531 Steinberg, D.K., and Benway, H.M. : Towards a transformative understanding
532 of the ocean's biological pump: priorities for future research. Report on the
533 NSF Biology of the Biological Pump Workshop. Ocean Carbon and

Biogeochemistry (OCB) Program, Woods Hole, MA http://dx.doi.org/10.1575/1912/8263, 2016.

Burd, A.B., and Jackson, G.A. :Particle aggregation. Annu. Rev. Mar. Sci. 1:65–90. http:// dx.doi.org/10.1146/annurev.marine.010908.163904, 2009.

Claquin, P., Probert, I., Lefebvre, S., and Veron, B. :Effects of temperature on photosynthetic parameters and TEP production in eight species of marine microalgae. Aquat. Microb. Ecol. 51:1–11. http://dx.doi.org/10.3354/ame01187, 2008.

Corzo A, Rodriguez-Galvez, S., Lubian, L., Sangrá, P., Martínez, A., and Morillo, J.A. : Spatial distribution of transparent exopolymer particles in the Bransfield Strait, Antarctica. Journal of Plankton Research. 27(7): 635-646. https://doi.org/10.1093/plankt/fbi038, 2005.

Corzo, A., Morillo, J.A. and Rodríguez, S. : Production of transparent exopolymer particles (TEP) in cultures of Chaetoceroscalcitrans under nitrogen limitation. Aquat. Microb. Ecol. 23, 63–72, 2000.

Cunliffe, M., Engel, A., Frka, S., Gašparović, B., Guitart, C., Murrell, J.C., Salter, M., Stolle, C., Upstill-Goddard, R., and Wurl, O. : Sea surface microlayers: a unified physicochemical and biological perspective of the air-ocean interface. Prog. Oceanogr. 109: 104–116. http://dx.doi.org/10.1016/j.pocean.2012.08.004, 2013.

Engel, A, and Passow, U.: Carbon and nitrogen content of transparent exopolymer particles (TEP) in relation to their Alcian Blue adsorption. Marine Ecology Progress Series. 2001; 219: 1-10. https://doi.org/10.3354/meps219001, 2001.

Engel, A.: The role of transparent exopolymer particles (TEP) in the increase in apparent particle stickiness during the decline of a diatom bloom. Journal of Plankton Research. 22(3): 485-497. https://doi.org/10.1093/plankt/22.3.485, 2000.

Engel, A.: Direct relationship between CO2 uptake and transparent exopolymer particles production in natural phytoplankton. Journal of Plankton Research. 24(1): 49-53. https://doi.org/10.1093/plankt/24.1.49, 2002.

563 Engel, A.: Distribution of transparent exopolymer particles (TEP) in the northeast
564 Atlantic Ocean and their potential significance for aggregation processes.
565 Deep Sea Research I. 51(1): 83-92. https://doi.org/10.1016/j.dsr.2003.09.001,
566 2004.

567 Fu, M.Z., Wang, Z.L., Li, Y., Li, R.X., Sun, P., Wei, X.H., Lin, X.Z., and Guo, J.S.:
568 Phytoplankton biomass size structure and its regulation in the Southern
569 Yellow Sea (China): seasonal variability. Cont. Shelf Res. 29 2178–2194,
570 2009.

571 Fukao, T, Kimoto, K., and Kotani, Y.: Effect of temperature on cell growth and
572 production of transparent exopolymer particles by the diatom Coscinodiscus
573 granii isolated from marine mucilage. Journal of Applied Phycology. 24: 181-
574 186. https://doi.org/10.1007/s10811-011-9666-3, 2012.

575 Garc, C., Prieto, L., Vargas, M., et al. Hydrodynamics and the spatial distribution of
576 plankton and TEP in the Gulf of Cádiz (SW Iberian Peninsula), Journal of
577 Plankton Research, 24 : 817-833, 2002.

578 Guo, S.J., Feng, Y.Y., Wang, L., Dai, M.H., Liu, Z.L., Bai, Y., Sun, J.: Seasonal variation
579 in the phytoplankton community of a continental-shelf sea: The East China
580 Sea. Marine Ecology Progress Series. 516: 103-126.
581 https://doi.org/10.3354/meps10952, 2014.

582 Guo, S., and Sun, X.: Carbon biomass, production rates and export flux of copepods fecal
583 pellets in the Changjiang (Yangtze) River estuary. Journal of Oceanology and
584 Limnology, 36(4), 1244–1254. doi:10.1007/s00343-018-7057-1, 2018.

585 Hong Y, Smith, W.O., and White, A.M.: Studies on transparent exopolymer particles
586 (TEP) produced in the Ross Sea (Antarctica)and by Phaeocystisantarctica
587 (Prymnesiophyceae). J Phycol.33:368–376, 1997.

588 Huang, C. J., Dong, Q.X., and Lin J.D.: Impact of global change on marine fisheries and
589 adaptation options. Journal of Oceanography in Taiwan Strait, 18(4): 481-494,
590 1999. (in Chinese with English abstract)

591 Hwang, J.H., Van, S. P., Choi, B.-J., Chang, Y. S., and Kim, Y. H.: The Physical
592 Processes in the Yellow Sea, Ocean & Coastal Management, 102 (2014), 449-
593 57, 2014.

594 Isobe, A.: Recent advances in ocean-circulation research on the Yellow Sea and East
595 China Sea shelves. J. Oceanagr. 64, 569e584, 2008.

596 Iversen, M.H., and Robert, M.L.: Ballasting effects of smectite on aggregate formation
597 and export from a natural plankton community. Mar. Chem. 175:18–27.
598 http://dx.doi.org/ 10.1016/j.marchem.2015.04.009, 2015.

599 Javier, R., Carlos, M.G., and Jaime, R.: Sedimentation loss of phytoplankton cells from
600 the mixed layer: effects of turbulence levels. Journal of Plankton Research.
601 18(9): 1727-1734. https://doi.org/10.1093/plankt/18.9.1727 , 1996.

602 Jokulsdottir, T., and Archer D.: A stochastic, Lagrangian model of sinking biogenic
603 aggregates in the ocean (SLAMS 1.0): model formulation, validation and
604 sensitivity. Geosci. Model Dev. 9. http://dx.doi.org/10.5194/gmd-9-1455-
605 2016, 2016.

606 Kodama T., Kurogi, H., Okazaki, M., Jinbo, T., and others.: Vertical distribution of
607 transparent exopolymer particle (TEP) concentration in the oligotrophic
608 western tropical North Pacific. Mar Ecol Prog Ser 513:29-37.
609 https://doi.org/10.3354/meps10954, 2014

610 Li, X., Feng, Y., Leng, X., Liu, H., and Sun, J.: Phytoplankton species composition of
611 four ecological provinces in Yellow Sea, China. Journal of Ocean University
612 of China, 16(6), 1115–1125. doi:10.1007/s11802-017-3270-3, 2017.

613 Lili, M. A., Chen, M., Guo, L., Lin, F., and Tong, J.: Distribution and source of
614 transparent exopolymer particles in the northern bering sea. Acta
615 Oceanologica Sinica, 34(5), 81-90, 2012.

616 Liu, H., Huang, Y., Zhai, W., Guo, S., Jin, H., and Sun, J.: Phytoplankton communities
617 and its controlling factors in summer and autumn in the southern Yellow Sea,
618 China. Acta Oceanologica Sinica, 34(2), 114–123. doi:10.1007/s13131-015-
619 0620-0, 2015a.

620 Liu, X., Huang, B., Huang, Q., Wang, L., Ni, X., Tang, Q., … Sun, J.: Seasonal
621 phytoplankton response to physical processes in the southern Yellow Sea.
622 Journal of Sea Research, 95, 45–55. doi: 10.1016/j.seares.2014.10.017, 2015b

623 Logan, B.E., Passow, U., Alldredge, A.L., Grossartt, H.P., and Simont, M.: Rapid
624 formation and sedimentation of large aggregates is predictable from
625 coagulation rates (halflives) of transparent exopolymer particles (TEP). Deep-
626 Sea Res. II 42 203–214, 1995.

627 Malpezzi, M.A， Sanford, L.P., and Crump, B.C.: Abundance and distribution of
628 transparent exopolymer particles in the estuarine turbidity maximum of
629 Chesapeake Bay.Marine Ecology Progress Series， 486： 23-35, 2013.

630 Mari, X.: Does ocean acidification induce an upward flux of marine aggregates[J]？
631 Biogeosciences， 5（4）： 1023-1031, 2008.

632 Mari, X., Rassoulzadegan, F., Brussaard, C.R.D., and Wassmann, P.: Dynamics of
633 transparent exopolymeric particles (TEP) production by Phaeocystisglobosa
634 under N- or Plimitation: a controlling factor of the retention/export balance.
635 Harmful Algae 4: 895–914. http://dx.doi.org/10.1016/j.hal.2004.12.014, 2005.

636 Mari, X., Passow, U., Migon, C., Burd, A.B., and Legendre, L.: Transparent exopolymer
637 particles: Effects on carbon cycling in the ocean. Progress in Oceanography,
638 151, 13–37. doi:10.1016/j.pocean.2016.11.002, 2017.

639 Mari, X., J.P. Torréton, C.B.T. Trinh, T. Bouvier, C.V. Thuoc, J.P. Lefebvre, and
640 S.Ouillon.: Aggregation dynamics along a salinity gradient in the Bach Dang
641 estuary, North Vietnam. Estuarine, Coastal and Shelf Science. 96: 151-158.
642 https://doi.org/10.1016/j.ecss.2011.10.028, 2012.

643 Mopper, K., Zhou, J., Sri Ramana, K., Passow, U., Dam, H.G., and Drapeau, D.T.: The
644 role of surface-active carbohydrates in the flocculation of a diatom bloom in a
645 mesocosm. Deep-Sea Res. II Top. Stud. Oceanogr. 42:47–73.
646 http://dx.doi.org/10.1016/0967- 0645(95)00004-A, 1995.

647 Mopper, K., Zhou, J., Sri Ramana, K., Passow, U., Dam, H.G., and Drapeau, D.T.: The
648 role of surface-active carbohydrates in the flocculation of a diatom bloom in a

649 mesocosm. Deep-Sea Res. II Top. Stud. Oceanogr. 42:47–73.
650 http://dx.doi.org/10.1016/0967- 0645(95)00004-A, 1995.

651 Naimie, C.E., Blain, C.A., and Lynch, D.R.: Seasonal mean circulation in the Yellow Sea
652 — a model-generated climatology. Continental Shelf Research 21(6-7), 667–
653 695. doi:10.1016/s0278-4343(00)00102-3, 2001.

654 Obernosterer. I., and Herndl, G.J.: Phytoplankton extracellular release and bacterial
655 growth: dependence on inorganic N: P ratio. Marine Ecology Progress
656 Series.116: 247-257. https://doi.org/10.3354/meps116247, 1995.

657 Orellana, M.V., Matrai, P.A., and Leck, C., Rauschenberg, C.D., Lee, A.M., and Coz, E.:
658 Marine microgels as a source of cloud condensation nuclei in the high arctic.
659 Proc. Natl. Acad. Sci. U. S. A. 108, 13612–13617, 2011.

660 Ortega-Retuerta, E., Duarte, C.M., and Reche, I.: Significance of Bacterial Activity for
661 the Distribution and Dynamics of Transparent Exopolymer Particles in the
662 Mediterranean Sea. Microbial Ecology, 59(4), 808–818. doi:10.1007/s00248-
663 010-9640-7, 2010.

664 Ortega-Retuerta, E., Mazuecos, I.P., Reche, I., Gasol, J.M., Álvarez-Salgado, X.A.,
665 Álvarez, M., Montero, M.F., Arístegui, J.: Transparent Exopolymer Particle
666 (TEP) distribution and in situ prokaryotic generation across the deep
667 Mediterranean Sea and nearby North East Atlantic Ocean, Progress in
668 Oceanography, doi: https://doi.org/10.1016/j.pocean.2019.03.002, 2019.

669 Ortega-Retuerta, E., Reche, I., Pulida-Villena, E., et al.: Uncoupled distributions of
670 transparent exopolymer particles (TEP) and dissolved carbohydrates in the
671 Southern Ocean.Marine Chemistry,115： 59-65, 2009.

672 Parinos, C., Gogou, A., Krasakopoulou, E., Lagaria, A., Giannakourou, A., Karageorgis,
673 A. P., & Psarra, S.: Transparent Exopolymer Particles (TEP) in the NE
674 Aegean Sea frontal area: Seasonal dynamics under the influence of Black Sea
675 water. Continental Shelf Research, 149, 112–123.
676 doi:10.1016/j.csr.2017.03.012, 2017.

677 Passow, U.: Production of transparent exopolymer particles (TEP) by phyto- and
678 bacterioplankton. Mar. Ecol. Prog. Ser. 236:1–12. http://dx.doi.org/10.3354/
679 meps236001, 2002a.

680 Passow, U.: Transparent exopolymer particles (TEP) in aquatic environments. Prog.
681 Oceanogr. 55 287–333, 2002b.

682 Passow, U., Alldredge, A.L., and Logan, B.E.: The role of particulate carbohydrate
683 exudates in the flocculation of diatom blooms. Deep-Sea Res. I Oceanogr.
684 Res. Pap. 41:335–357. http://dx.doi.org/10.1016/0967-0637(94)90007-8,
685 1994.

686 Passow, U., and Alldredge, A.L.: Distribution, size and bacterial-colonization of
687 transparent exopolymer particles (Tep) in theocean. Mar Ecol Prog Ser
688 113:185–198, 1994.

689 Passow, U., and Alldredge, A.L.: A dye-binding assay for the spectrophotometric
690 measurement of transparent exopolymer particles (TEP). Limnol. Oceanogr.
691 40, 1326–1335, 1995.

692 Passow, U., and Alldredge, A.L.: Do transparent exopolymer particles (TEP) inhibit
693 grazing by the euphausidEuphausiapacifica. J. Plankton Res. 21, 2203–2217,
694 1999.

695 Passow, U., Shipe, R.F., Murray, A., Pak, D.K., Brzezinski, M.A., and Alldredge, A.L.:
696 The origin of transparent exopolymerparticles (TEP) and their role in the
697 sedimentation of particulatematter. Cont Shelf Res 21:327–346, 2001.

698 Peng, A.G., and Huang, Y.P.: Study on TEP and its relationships with Uranium, Thorium,
699 Polonium Isotopes in Jiulong Estuary. Journal of Xiamen University.46(1):
700 38-42, 2007. (in Chinese with English abstract)

701 Prairie, J.C., Ziervogel, K., Camassa, R., McLaughlin, R.M., White, B.L., Dewald, C.,
702 and Arnosti, C.: Delayed settling of marine snow: effects of density gradient
703 and particle properties and implications for carbon cycling. Mar. Chem.
704 175:28–38. http://dx.doi.org/ 10.1016/j.marchem.2015.04.006, 2015.

705 Prieto, L., Navarro, G., Cózar, A., Echevarría, F., and García, C.M.: Distribution of TEP
706 in the euphotic and upper mesopelagic zones of the southern Iberian coasts.

Deep Sea Research II. 53(11-13): 1314-1328. https://doi.org/10.1016/j.dsr2.2006.03.009, 2006.

Prieto, L., Ruiz, J., Echevarría, F., García, C.M., Bartual, A., Gálvez, J.A., Corzo, A., and Macías, D.: Scales and processes in the aggregation of diatom blooms: high time resolution and wide size range records in a mesocosm study. Deep Sea Research II. 49: 1233-1253. https://doi.org/10.1016/S0967-0637(02)00024-9, 2002.

Radić, T., Kraus, R., Fuks, D., Radić, J., and Pečar, O.: Transparent exopolymeric particles' distribution in the northern Adriatic and their relation to microphytoplankton biomass and composition. Science of The Total Environment, 353(1-3), 151–161. doi: 10.1016/j.scitotenv.2005.09.013, 2005.

Ramaiah, N., Takeda, S., Furuya, K., Yoshimura, T., and others.: Effect of iron enrichment on the dynamics of transparent exopolymer particles in the western subarctic Pacific. Prog Oceanogr 64:253−261, 2005.

Ramaiah, N., Yoshikawa, T., and Furuya, K.: Temporal variations in transparent exopolymer particles (TEP) associated with a diatom spring bloom in a subarctic ria in Japan. Marine Ecology Progress Series. 212: 79-88. https://doi.org/10.3354/meps212079, 2001.

Rochelle-Newall, E.J., Mari, X., and Pringault, O.: Sticking properties of transparent exopolymeric particles (TEP) during aging and biodegradation. Journal of Plankton Research. 32(10): 1433-1442. https://doi.org/10.1093/plankt/fbq060

Ruiz, J., Macías, D., and Peters, F.: Turbulence increases the average settling velocity of phytoplankton cells. Proceeding of the National Academy of Science of the United States of America. 101(51): 17720-17724. https://doi.org/10.1073/pnas.0401539101, 2004.

Stoderegger, K., and Herndl, G.J.: Production of exopolymer particles by marine bacterioplankton under contrasting turbulence conditions. Marine Ecology Progress Series. 189: 9-16. https://doi.org/10.3354/meps189009, 1999.

735 Su, J.: Circulation dynamics of the China seas: north of 181N. In: Robinson, A.R., Brink,
736 K., (Eds.), The Sea, vol. 11. The Global Coastal Ocean: Regional Studies and
737 Syntheses. Wiley, New York,pp. 483–506, 1999, 1998.

738 Sun, C.C., Wang, Y.S., Wu, M.L., Li, N., Lin, L., Song, H., Wang, Y.T., Deng, C., Peng,
739 Y.L., Sun, F.L., and Li, C.L.: Distribution of transparent exopolymer particles
740 in the Pearl River Estuary in summer. Journal of Tropical Oceanography.
741 29(5): 81-87, 2010. (in Chinese with English abstract)

742 Surosz, W., Palinska, K. A., and Rutkowska, A.: Production of Transparent Exopolymer
743 Particles (Tep) in the Nitrogen Fixing Cyanobacterium Anabaena Flos-*a*quae
744 Ol-K10, Oceanologia, 48 (3). pp. 385–394, 2006.

745 Tang, Q. S., Jin, X.S., Wang, J., Zhuang, Z.M., Cui, Y., and Meng, T.X.: Decadal-scale
746 variations of ecosystem productivity and control mechanisms in the Bohai
747 Sea. Fisheries Oceanography, 12(4-5): 223-233, 2003.

748 Tang, Q.S., and Su, J. L.: Marine Ecosystem Dynamics Study of China. Key Scientific
749 Questions and Developing Strategies (in Chinese). Beijing: Science Press, 3–
750 34, 2001.

751 Tang, Q.S., Su, J.L., and Zhang, J.: China GLOBEC II: a case study of the Yellow Sea
752 and East China Sea ecosystem dynamics preface. Deep-Sea Res. II 57, 993–
753 995, 2010.

754 Tang, Q.S., Su, J.L., Kishi, M.J., and Oh, I.S.: An introduction to the Second China–
755 Japan– Korea Joint GLOBEC Symposium on the ecosystem structure, food
756 web trophodynamics and physical-biological processes in the Northwest
757 Pacific. J. Mar. Syst. 67, 203–204, 2007.

758 Ter-Braak, C.J.F., and Šmilauer, P.: CANOCO Reference Manual and CanoDraw for
759 Windows User's Guide: Software for Canonical Community Ordination
760 (Version 4.5). Microcomputer Power, Wageningen. Soil macrofauna in
761 organic and conventional coffee plantations in Brazil, 2002.

762 Thuy, N.T., Lin, J.C.-T., Juang, Y., and Huang, C.: Temporal variation and interaction of
763 full size spectrum Alcian blue stainable materials and water quality parameters
764 in a reservoir. Chemosphere 131:139–148.
765 http://dx.doi.org/10.1016/j.chemosphere.2015.03.023, 2015.

766 Tranvik, L.J., Sherr, E.B., and Sherr, B.F.: Uptake and utilization of colloidal DOM by
767 heterotrophic flagellates in seawater. Mar EcolProg Ser 92:301–309, 1993.

768 Turner, J.T.: Zooplankton fecal pellets, marine snow and sinking phytoplankton blooms.
769 Aquatic Microbial Ecology. 27: 57-102. https://doi.org/10.3354/ame027057,
770 1993, 2002.

771 Turner, J.T.: Zooplankton fecal pellets, marine snow, phytodetritus and the ocean's
772 biological pump. Progress in Oceanography. 130: 205-248.
773 https://doi.org/10.1016/j.pocean.2014.08.005, 2015.

774 Verdugo, P., Alldredge, A.L., Azam, F., Kirchman, D.L., Passow, U., and Santschi, P.H.:
775 The oceanic gel phase: a bridge in the DOM-POM continuum. Mar. Chem. 92,
776 67–85, 2004.

777 Vicente Villardón, J.L. MULTBIPLOT: A package for Multivariate Analysis using
778 Biplots. Departamento de Estadística. Universidad de Salamanca, 2015.
779 (http://biplot.usal.es/ClassicalBiplot/index.html)

780 Vicente, I.D., Ortega-Retuerta, E., Romera, O., Moreles-Baquero, R., and Reche, I.:
781 Contribution of transparent exopolymer particles to carbon sinking flux in an
782 oligotrophic reservoir. Biogeochemistry. 96: 13-23.
783 https://doi.org/10.1007/s10533-009-9342-8, 2009.

784 Welschmeyer, N. A.: Fluorometric analysis of chlorophyll-a in the presence of
785 chlorophyll-b and pheopigments [J]. Limnology and Oceanography, 39 :
786 1985-1992, 1994 .

787 Wen, L., Sun, J., He, Q., Wang, D., and Wang, M.: Winter phytoplankton assemblages of
788 coastal Yellow Sea connected to Jiaozhou Bay, China. Journal of Ocean
789 University of China, 6(1), 40–46. doi:10.1007/s11802-006-0040-7, 2007.

790 Wetz, M. S., Robbins, M.C., and Paerl, H.W.: Transparent exopolymer particles (TEP)
791 in a river-dominated estuary: spatial and temporal distributions and an
792 assessment of controls upon TEP formation.Estuaries and Coasts, 32（3） :
793 447-455, 2009.

794 Wurl, O., and Holmes, M.: The gelatinous nature of the sea-surface microlayer. Mar.
795 Chem. 110:89–97. http://dx.doi.org/10.1016/j.marchem.2008.02.009, 2008.

796 Wurl, O., Wurl, E., Miller, L., Johnson, K., and Vagle, S.: Formation and global
797 distribution of sea-surface microlayers. Biogeosciences 8:121–135.
798 http://dx.doi.org/10. 5194/bg-8-121-2011, 2011a.

799 Wurl, O., Miller, L., and Vagle, S.: Production and fate of transparent exopolymer
800 particles in the ocean. J. Geophys. Res. C: Oceans 116, 2011b.

801 Wurl, O., Miller, L., Röttgers, R., and Vagle, S.: The distribution and fate of surface-
802 active substances in the sea-surface microlayer and water column. Mar. Chem.
803 115:1–9. http://dx.doi.org/10.1016/j.marchem.2009.04.007, 2009.

804 Xu, S., Song, J., Li, X., Yuan, H., Li, N., Duan, L., and Sun, P.: Changes in nitrogen and
805 phosphorus and their effects on phytoplankton in the Bohai Sea. Chinese
806 Journal of Oceanology and Limnology 28(4), 945–952. doi:10.1007/s00343-
807 010-0005-3, 2010.

808 Yang, G., Wu, Z., Song, L., and Lu, X.: Seasonal Variation of Environmental Variables
809 and Phytoplankton Community Structure and Their Relationship in Liaodong
810 Bay of Bohai Sea, China. Journal of Ocean University of China, 17(4), 864–
811 878. doi:10.1007/s11802-018-3407-z, 2018.

812 Yuan, D., Zhu, J., Li, C., and Hu, D.: Cross-shelf circulation in the Yellow and East
813 China Seas indicated by MODIS satellite observations. J. Mar. Syst. 70
814 (2008), 134e149, 2008.

815 Zang, J., Tang, Y., Zou E., and Lie, H.-J.: Analysis of Yellow Sea circulation. Chinese
816 Science Bulletin, 48(S1), 12–20. doi:10.1007/bf02900935, 2003.

817 Zetsche, E.-M., and Ploug, H.: Marine chemistry special issue: Particles in aquatic
818 environments: From invisible exopolymers to sinking aggregates. Mar. Chem.
819 175, 1–4, 2015.

820 Zhang, F., Li, C.L., Sun, S., Wu, Y.L., and Ren, J.P.: Distribution patterns of chlorophyll
821 a in spring and autumn in association with hydrological features in the
822 southern Yellow Sea and northern East China Sea. Chin. J. Oceanol. Limnol.
823 27, 784–792, 2009.

Zhang, S., Leng, X., Feng, Y., Ding, C., Yang, Y., Wang, J., … Sun, J.: Ecological provinces of spring phytoplankton in the Yellow Sea: species composition. Acta Oceanologica Sinica, 35(8), 114–125. doi:10.1007/s13131-016-0872-3, 2016.

Table 1 Average statuses of temperature (ºC), salinity (PSU), nutrients (µmol/l), chl-*a* (µg/l), TEP (µg Xeq. L^{-1}) and TEP_S (m d^{-1}) during study seasons.

Seasons	Seas	Temperature	Salinity	DIP	DIN	DSi	NH_4	NO_3	NO_2	Chl-*a*	TEP	TEP_S
Autumn (2014)	Bohai Sea	9.77±0.50	24.13±0.52	0.29±0.11	10.24±3.53	7.24±3.13	0.98±0.55	0.18±0.07	9.08±3.46	0.34±0.13	0.42±0.35	0.90±0.11
	North Yellow Sea	13.23±1.48	31.56±0.49	0.18±0.13	3.91±1.98	3.70±2.81	0.45±0.31	0.27±0.23	3.19±2.28	0.35±2.30	0.44±0.65	0.95±0.11
	South Yellow Sea	16.32±3.32	31.60±0.75	0.22±0.22	4.95±3.23	5.64±3.14	0.58±0.19	0.16±0.24	4.21±3.24	0.78±0.43	0.93±.26	1.13±0.21
Summer (2015)	Bohai Sea	23.90±2.40	30.55±0.54	0.08±0.04	3.94±2.86	3.91±1.43	0.85±0.54	0.63±0.66	2.45±2.26	1.02±0.68	1.02±2.98	1.01±0.15
	North Yellow Sea	20.40±5.56	31.71±0.33	0.14±0.12	2.01±1.86	2.55±1.39	0.53±0.45	0.27±0.46	1.21±1.55	0.83±1.28	0.83±1.51	1.06±0.36
	South Yellow Sea	21.40±6.51	31.28±1.07	0.19±0.19	4.15±3.25	4.01±3.51	0.57±0.42	0.23±0.30	3.35±3.18	1.42±2.73	1.42±2.54	1.05±0.33
Winter (2015)	Bohai Sea	0.29±0.00	6.43±0.00	0.29±0.11	4.28±10.21	4.28±1.93	1.78±5.19	0.19±0.20	2.31±5.18	4.82±0.08	4.82±4.42	1.02±0.40
	North Yellow Sea	4.73±2.02	32.20±0.17	0.14±0.16	1.06±1.18	3.50±1.10	0.47±0.71	0.09±0.11	0.49±0.65	7.00±0.38	7.00±6.20	1.03±0.20

Table 2. Concentration of TEP in 0-50m depths at different area from various reports.

Location		TEP (μg Xeq. L^{-1})	References
Seas	Ross Sea	1003	Hong et al. (1997)
	The Baltic Sea	145-322	Engel (2002)
	Adriatic Sea	4-14800	Radic et al. (2005)
	Arabian Sea	507-560	Prieto et al. (2006)
	Weddell Sea	0-48.9	Ortega-Retuerta et al. (2009)
	Mediterranean Sea	19.4-53.1	Ortega-Retuerta et al. (2010)
	Eastern Mediterranean Sea	116-420	Bar-Zeev et al. (2011)
	North Yellow Sea	0.19-23.20	This Study (2014-15)
	South Yellow Sea	0.19-11.99	This Study (2014-15)
Part of Oceans	Northeast Atlantic	20-60	Engel (2004)
	Northwest Atlantic	10-120	Engle (2004)
	Santa Barbara Low Strait	85-252	Passow and Alldredge (1995)
	Western subarctic North Pacific	40-190	Ramaiah et al. (2005)
	Eastern tropical North Pacific	22.5	Wurl et al. (2011b)
	Eastern subarctic North Pacific	28.7	Wurl et al. (2011b)
	Western tropical North Pacific	43.3	Kodama et al. (2014)
Estuaries	Pearl River Estuary	85-1235	Sun et al. (2010)
	Jiulong river estuary	530-720	Peng and Huang (2007)
	Changjiang Estuary	173.33-1423.33	Guo & Sun (2018)
	Newson Estuary	805-1801	Wetz et al. (2009)
Bays	Gulf of Aqaba	130-222	Bar-Zeev et al. (2009)
	Gulf of Cadiz	25-717	Garc et al. (2002)
	Chesapeake Bay	37-2820	Malpezzi et al. (2013)
	Bohai Sea	0.19-14.75	This Study (2014-15)

Table 3. Concentration of TEP in 50-100 depths at different area from various reports.

Location		TEP (μgXeq. L^{-1})	References
Bays	Bransfield Strait	0-346	Corzo et al. (2005)
	Gulf of Aqaba	106-228	Bar-Zeev e.t al. (2009)
	Bohai Sea	0.39-4.33	This Study (2014-15)
Part of Oceans	Eastern tropical North Pacific	9.2	Wurl et al. (2011b)
	Eastern subarctic North Pacific	11.6	Wurl et al. (2011b)
	Western tropical North Pacific	42.2	Kodama et al. (2014)
Seas	Mediterranean Sea	9.1-94.3	Ortega-Retuerta et al. (2010)
	Eastern Mediterranean Sea	48-189	Bar-Zeev et al. (2011)
	North Yellow Sea	0.19-11.01	This Study (2014-15)
	South Yellow Sea	0.2-0.79	This Study (2014-15)

Table 5. Seasonal average TEP distribution in surface area from various research with their minimum to maximum ranges.

Seasons	Location	TEP (µg Xeq. L^{-1})	References
Autumn	Aegean Sea	42.1	Parinos et al. 2017
	Bohai Sea	0.42	This Study (2014-15)
	North Yellow Sea	0.44	This Study (2014-15)
	South Yellow Sea	0.93	This Study (2014-15)
Spring	Changjiang Estuary	506.67	Guo & Sun (20180
	Aegean Sea	93.3	Parinos et al. 2017
	Northeast coast of Japan	1021.50	Ramaiah et al. (2001)
	Southern Iberian coasts	533.50	Prieto et al. (2006)
Summer	Changjiang Estuary	948.33	Guo & Sun (2018)
	Baltic Sea	233.50	Engel (2002)
	Aegean Sea	81.1	Parinos et al. 2017
	Northeast Atlantic Ocean	65.00	Engel (2004)
	Bransfield Strait	173.00	Corzo et al. (2005)
	Jiulong estuary	625.00	Peng and Huang (2007)
	Pearl River estuary	660.00	Sun et al. (2010)
	Bohai Sea	1.02	This Study (2014-15)
	North Yellow Sea	0.83	This Study (2014-15)
	South Yellow Sea	1.42	This Study (2014-15)
Winter	Bohai Sea	4.82	This Study (2014-15)
	North Yellow Sea	7.00	This Study (2014-15)

Table 5. Seasonal average sedimentation rates of TEP in different locations with their maximum and minimum ranges from different reports.

Seasons	Location	TEPs (mD^{-1})	References
Autumn	Bohai Sea	0.90	This Study (2014-15)
	North Yellow Sea	0.95	This Study (2014-15)
	South Yellow Sea	1.13	This Study (2014-15)
Spring	Changjiang Estuary	0.33	Guo & Sun (2018)
	Santa Barbara Strait	-0.22 ~0.04	Azetsu-Scott and Passow (2004)
Summer	Changjiang Estuary	0.59	Guo & Sun (2018)
	Bohai Sea	1.01	This Study (2014-15)
	North Yellow Sea	1.06	This Study (2014-15)
	South Yellow Sea	1.05	This Study (2014-15)
Winter	South Pacific Ocean	-0.29 ~0.49	Mari (20080
	Bohai Sea	1.02	This Study (2014-15)
	North Yellow Sea	1.03	This Study (2014-15)

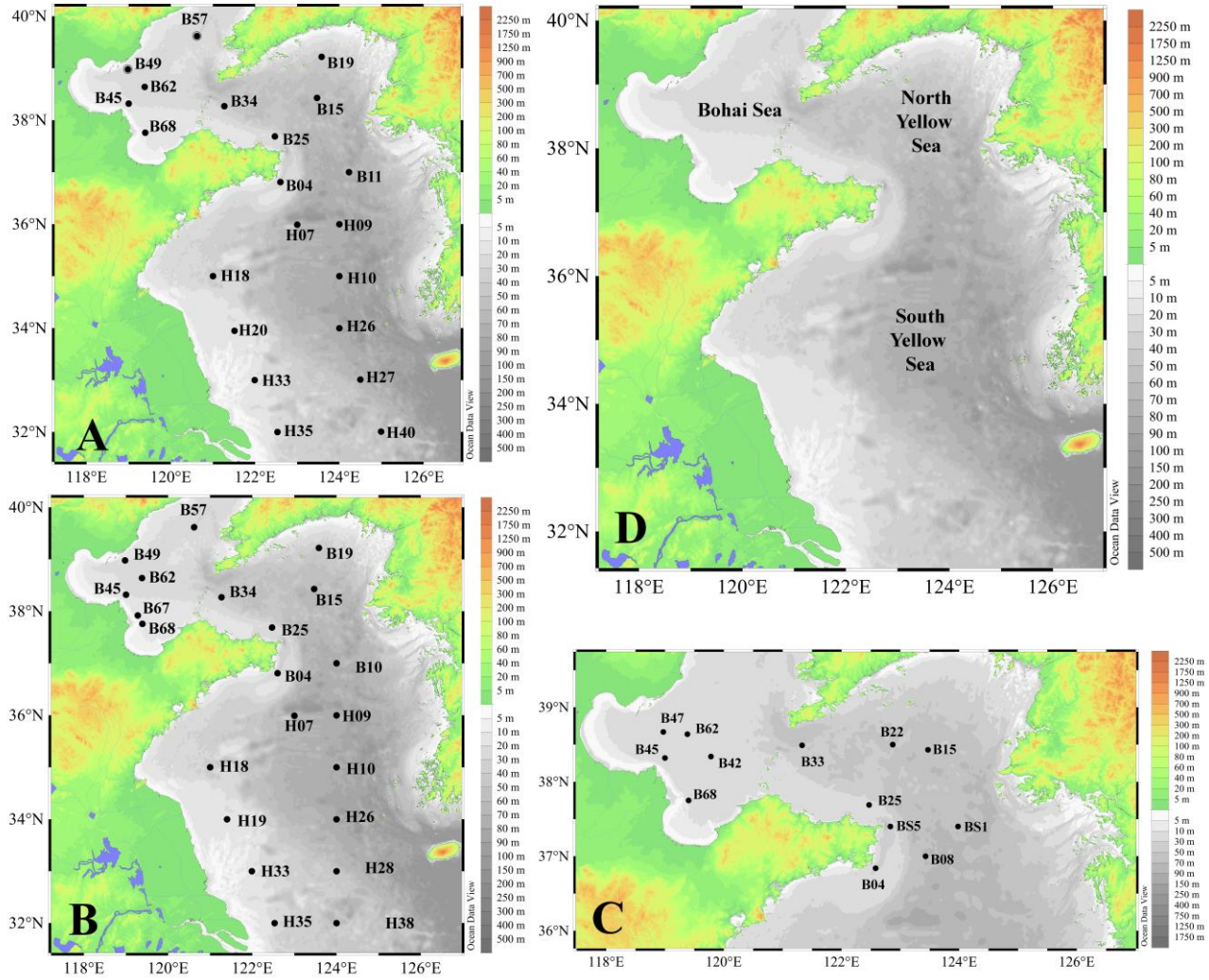

Figure 1. Study stations in map of autumn 2014 (A), summer 2015 (B) and winter 2015 (C) with their oceanic segmentation (D).

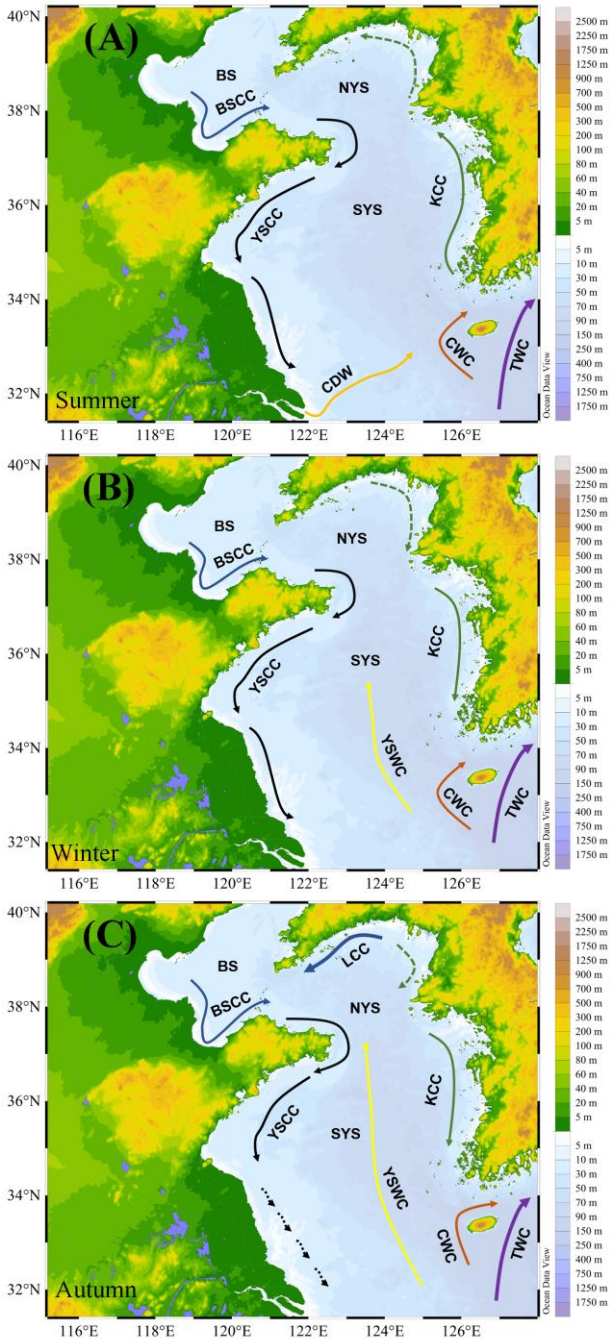

Figure 2. Direction of Currents at Bohai Sea (BS=Bohai Sea, BSCC=Bohai Sea coastal current), North Yellow Sea (NYS=North Yellow Sea, KCC=Korean Costal Current, LCC=Liaonan coastal current, YSCC=Yellow Sea Costal Current) and South Yellow Sea (SYS=South Yellow Sea, YSWC=Yellow Sea Warm Sea, CDW=Changiang Diluted Water, CWC= Cheju Warm Current, TWC=Tsushima Warm Current) during summer (a), winter (b) and autumn (c) seasons (Collaboratively modified after Hwang et al. 2014; Su 1998; Yuan et al. 2008; Isobe 2008, Zhang et al. 2003).

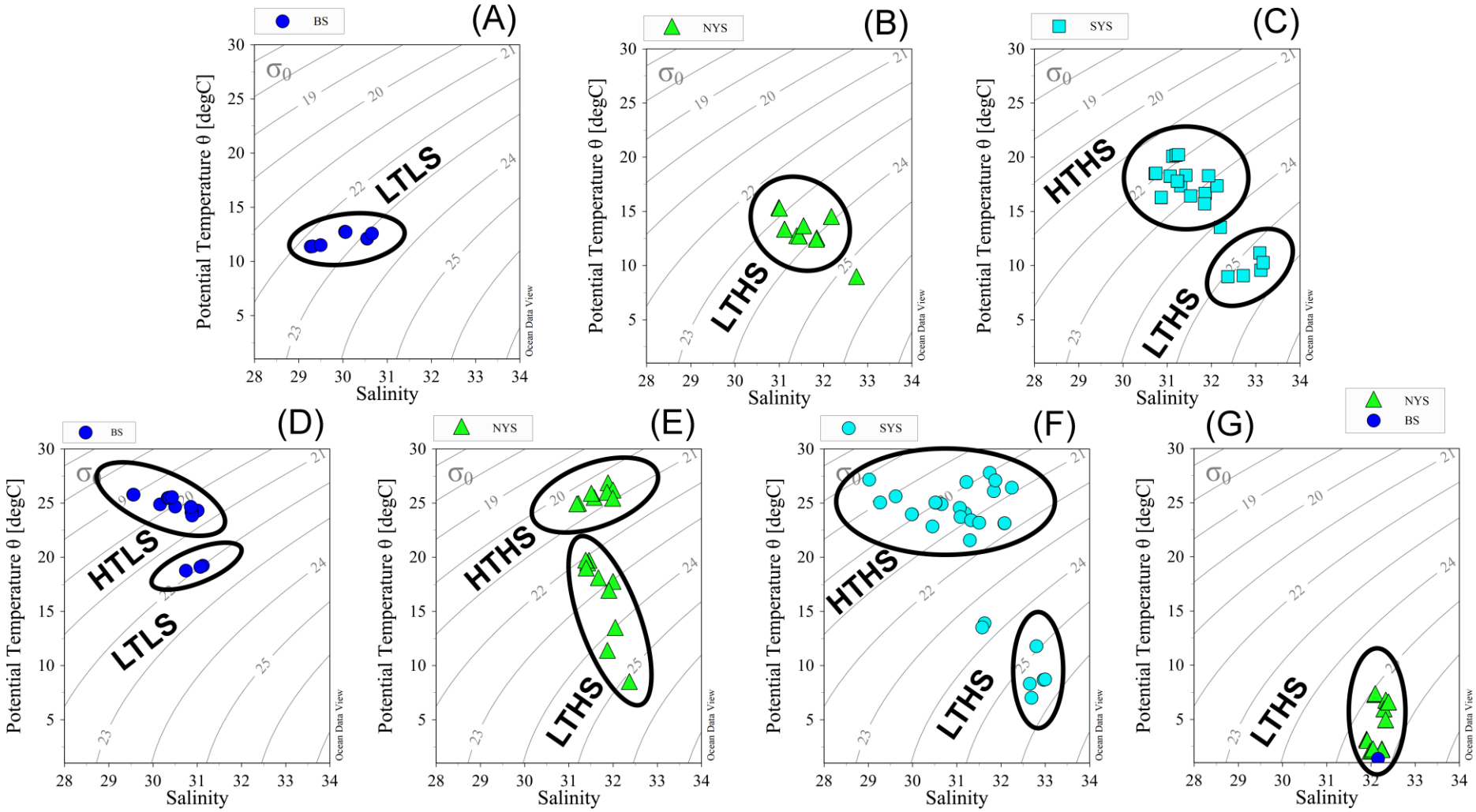

Figure 3. Density based seasonal water masses during autumn (A, B, C), summer (D, E, F) and winter (G) of BS (A, D, G), NYS (B, E, G) and SYS (C, F).

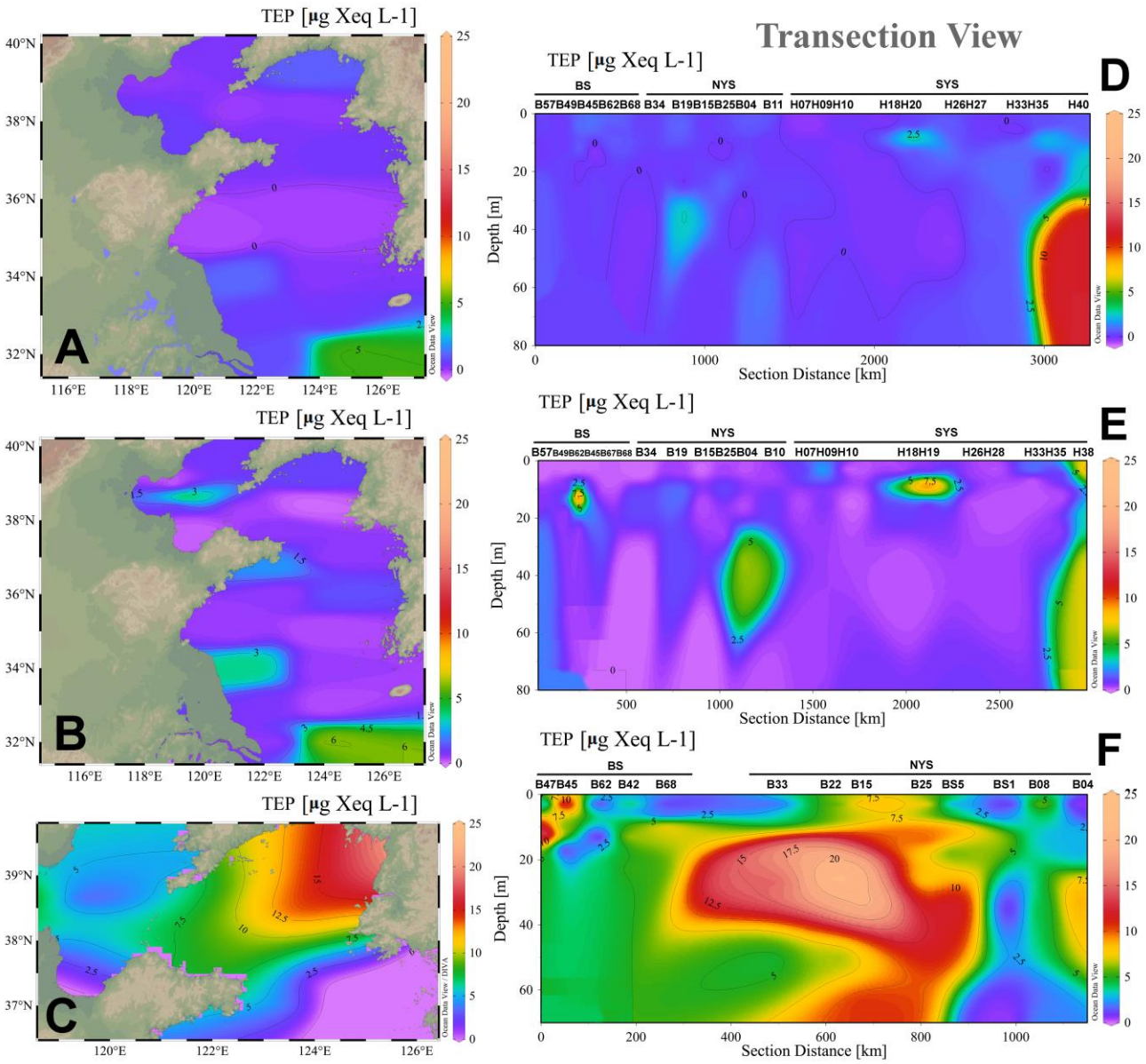

Figure 4. Average seasonal concentrations of TEP (A, B & C) with sectional view (D, E & F) of BS (D), NYS (E) and SYS (F) during autumn (A), summer (B) and winter (C).

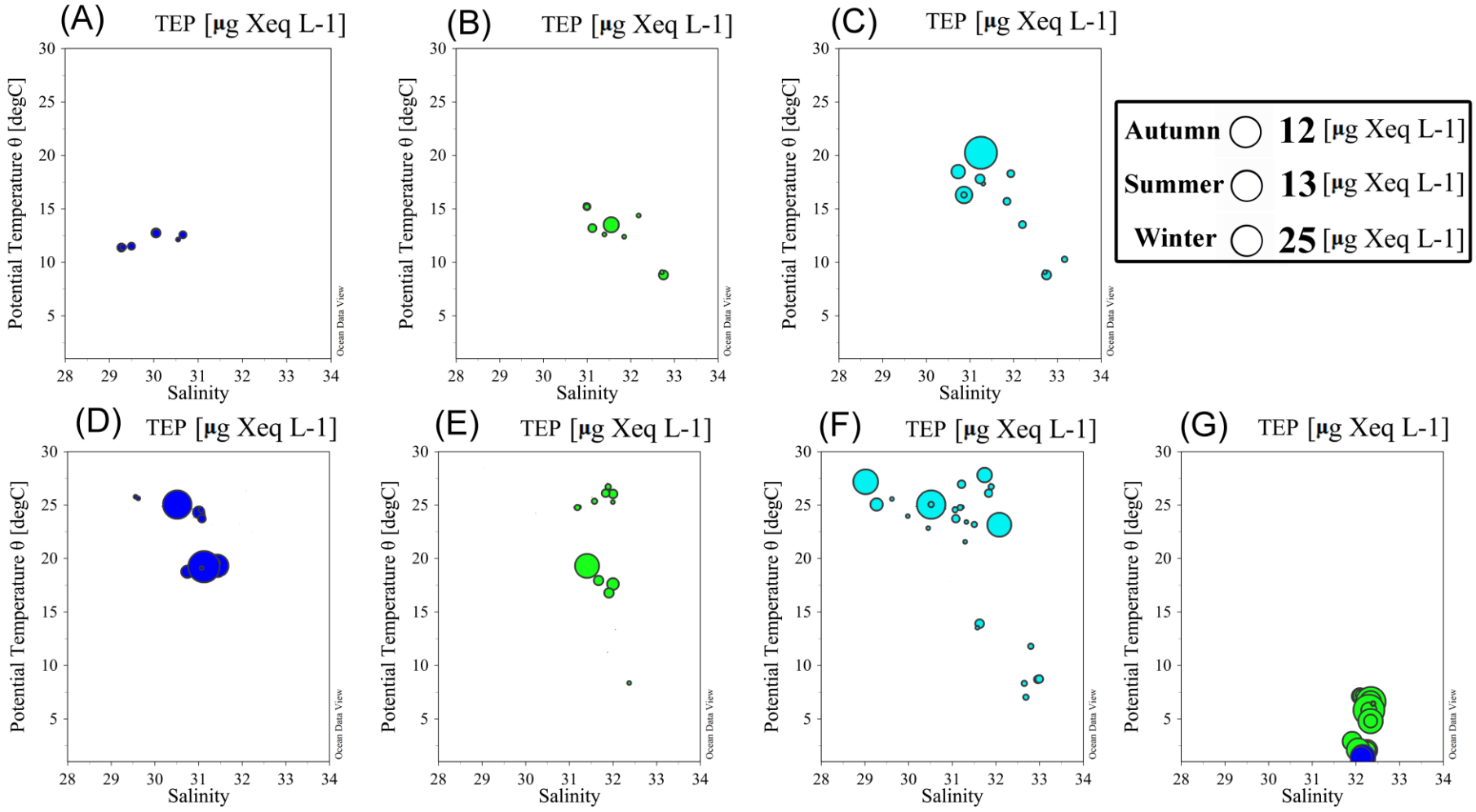

Figure 5. Seasonal TEP aggregations at different water mass during autumn (A, B, C), summer (D, E, F) and winter (G) of BS (A, D, G), NYS (B, E, G) and SYS (C, F).

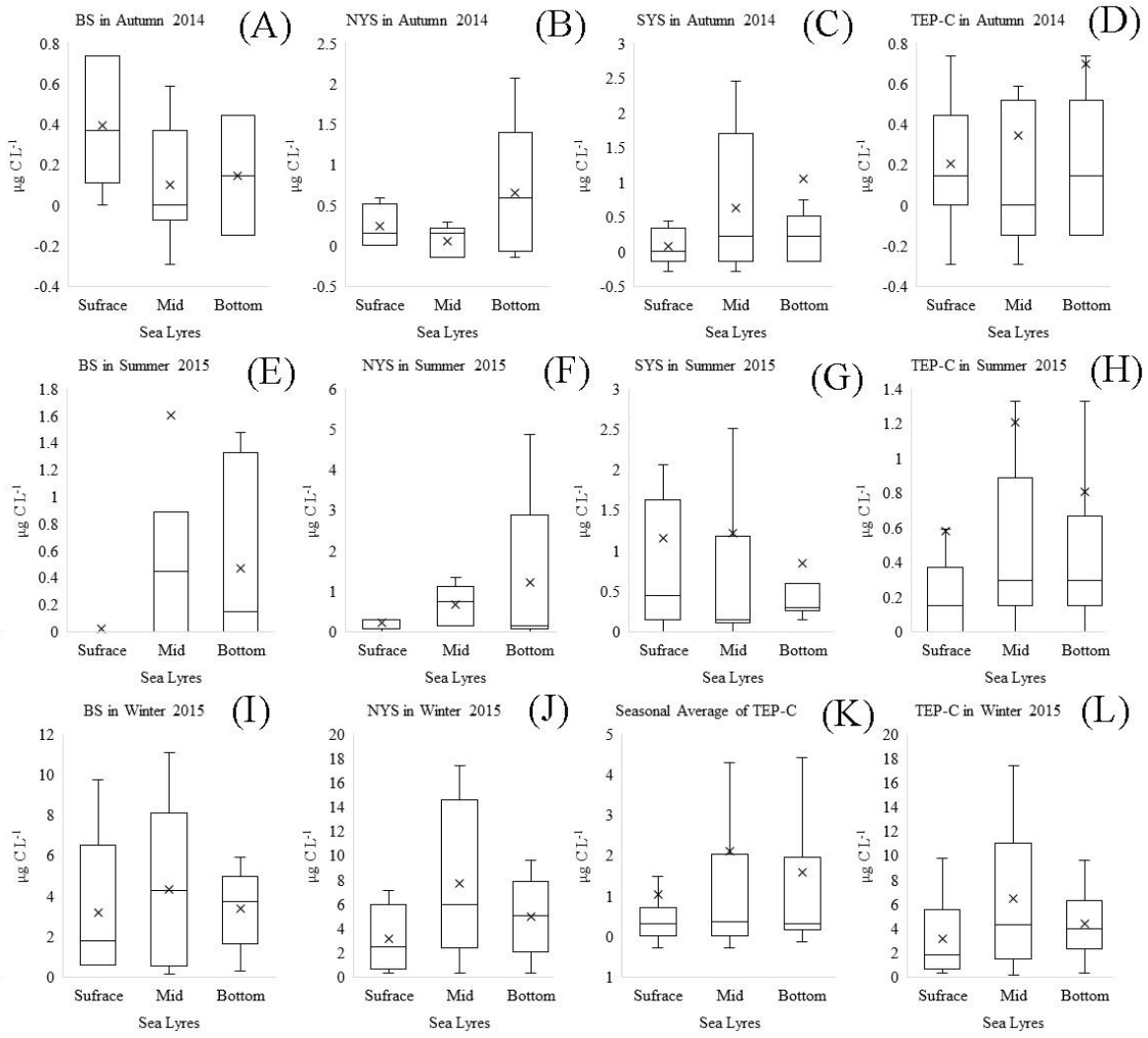

Figure 6. TEP associated carbon concentration during all seasons in Bohai Sea (A=autumn 2014, E=summer 2015, I=winter 2015), North Yellow Sea (B=autumn 2014, F=summer 2015, J=winter 2015), South Yellow Sea (C=Autumn 2014, G=summer 2015) with all data in average (K), autumn 2014 (D), summer 2015 (H) and winter 2015(L).

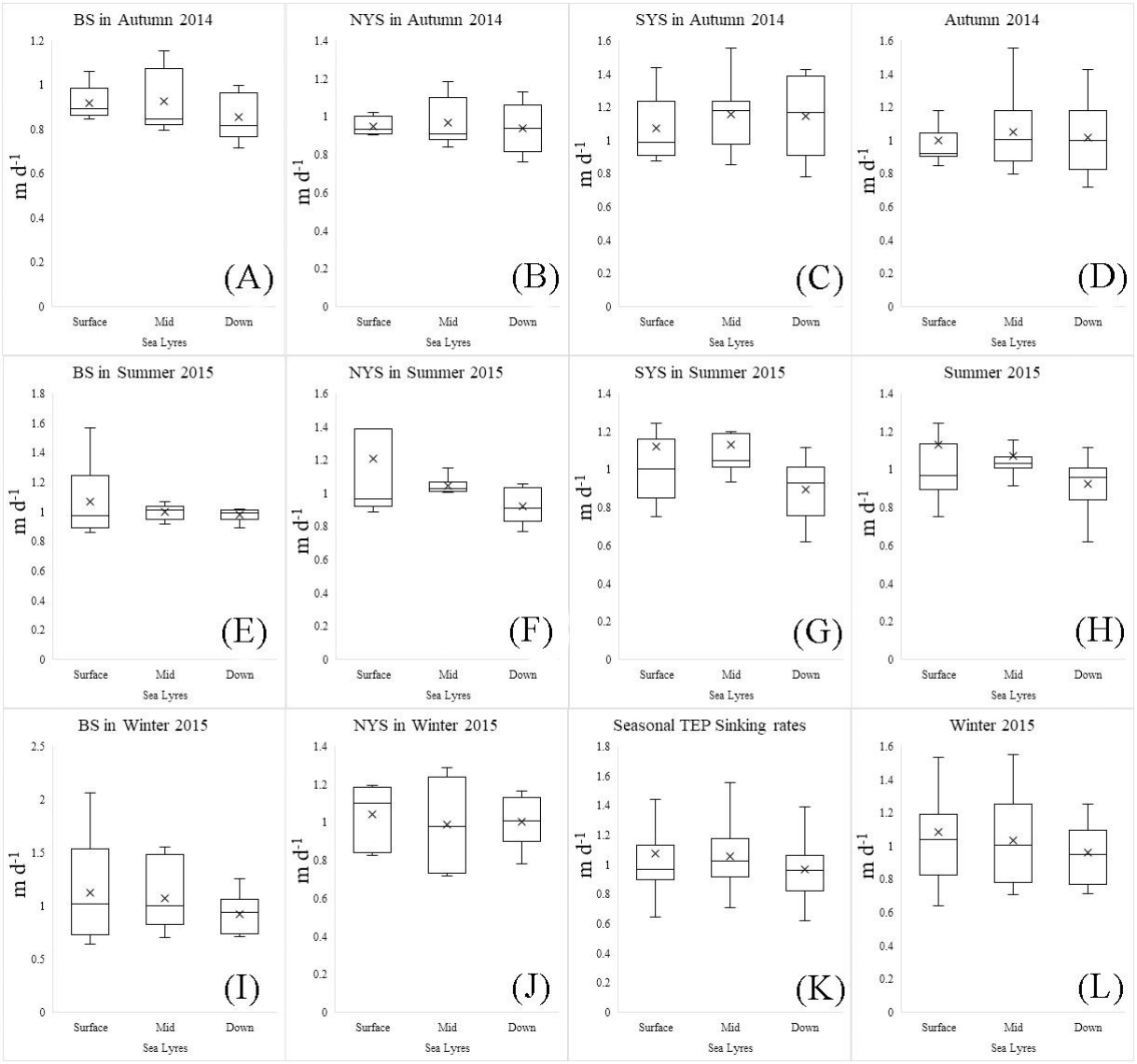

Figure 7. TEP sinking flux during all seasons in Bohai Sea (A=autumn 2014, E=summer 2015, I=winter 2015), North Yellow Sea (B=autumn 2014, F=summer 2015, J=winter 2015), South Yellow Sea (C=autumn 2014, G=summer 2015) with all seasonal sinking data in average (K), autumn 2014 (D), summer 2015 (H) and winter 2015(L).

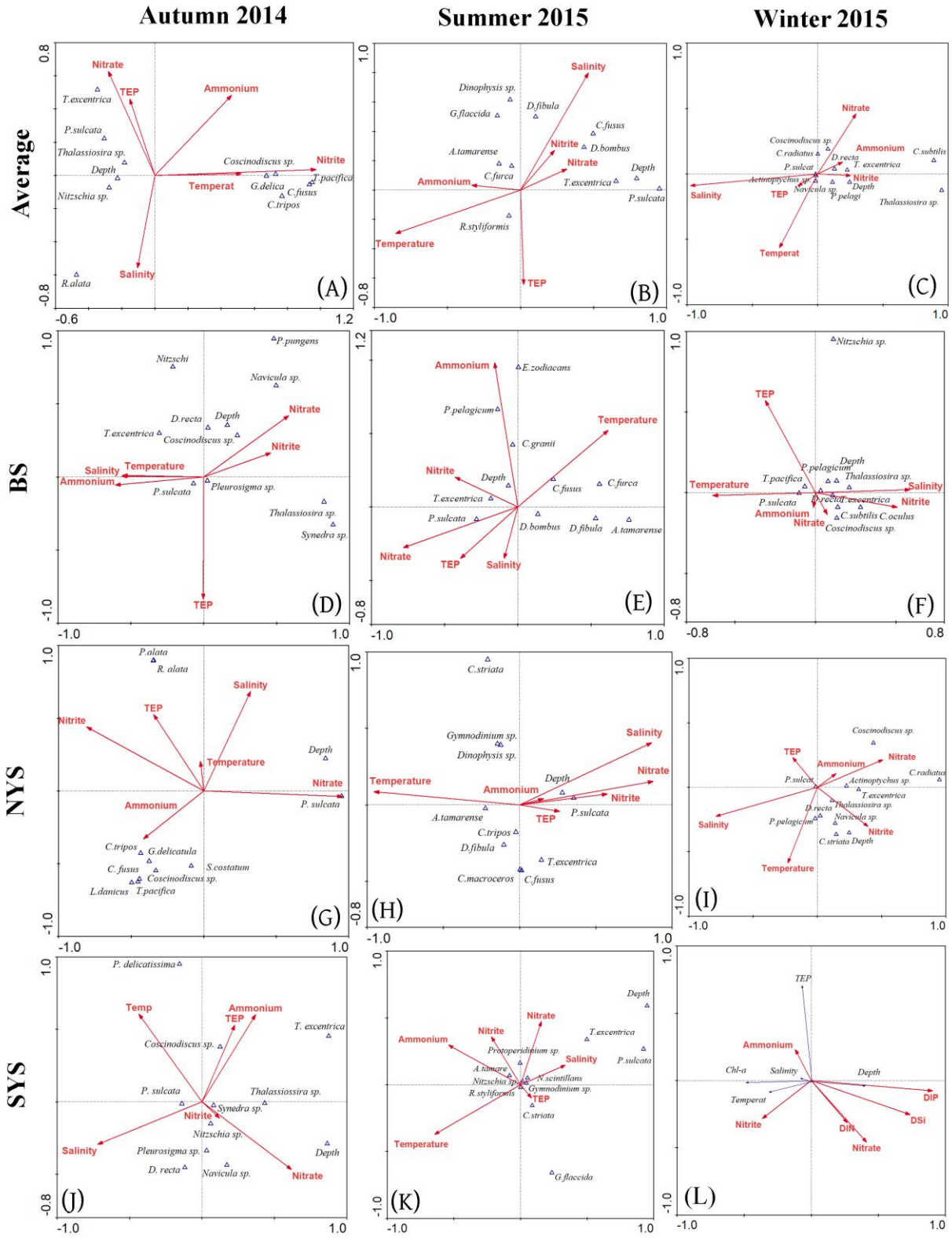

Figure 8. CCA analysis among biotic and abiotic parameters of all study areas. Seasonal average i.e. autumn 2014 (A), summer 2015 (B), winter 2015(C) and total (L) with the CCA of all parameters according to locations i.e. Bohai Sea (D=autumn 2014, E=summer 2015,

F=winter 2015), North Yellow Sea (G=Autumn 2014, H=summer 2015, I=winter 2015) and South Yellow Sea (J=autumn 2014, K=summer 2015).

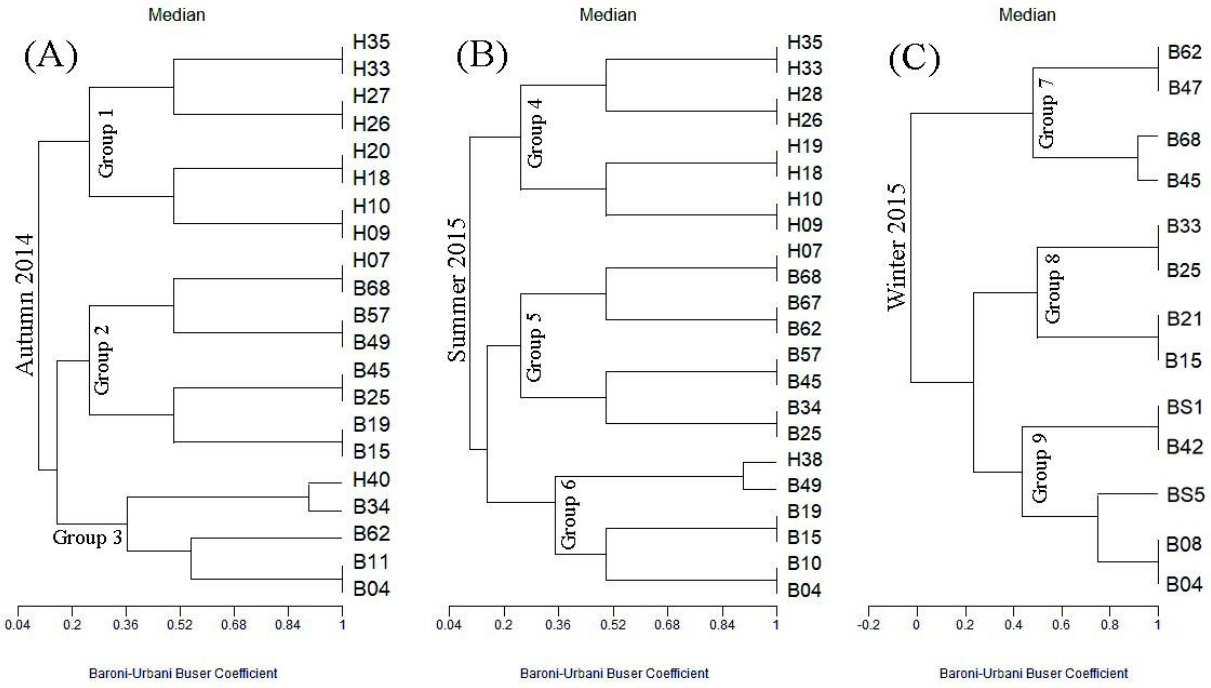

Figure 9. Seasonal Cluster analysis among related study stations of study area by considering all parameters and TEP, segmented by seasons i.e. autumn 2014 (A), summer 2015 (B) and

winter 2015 (C). Groups (1-9) are indicating clustered group of closely related stations.

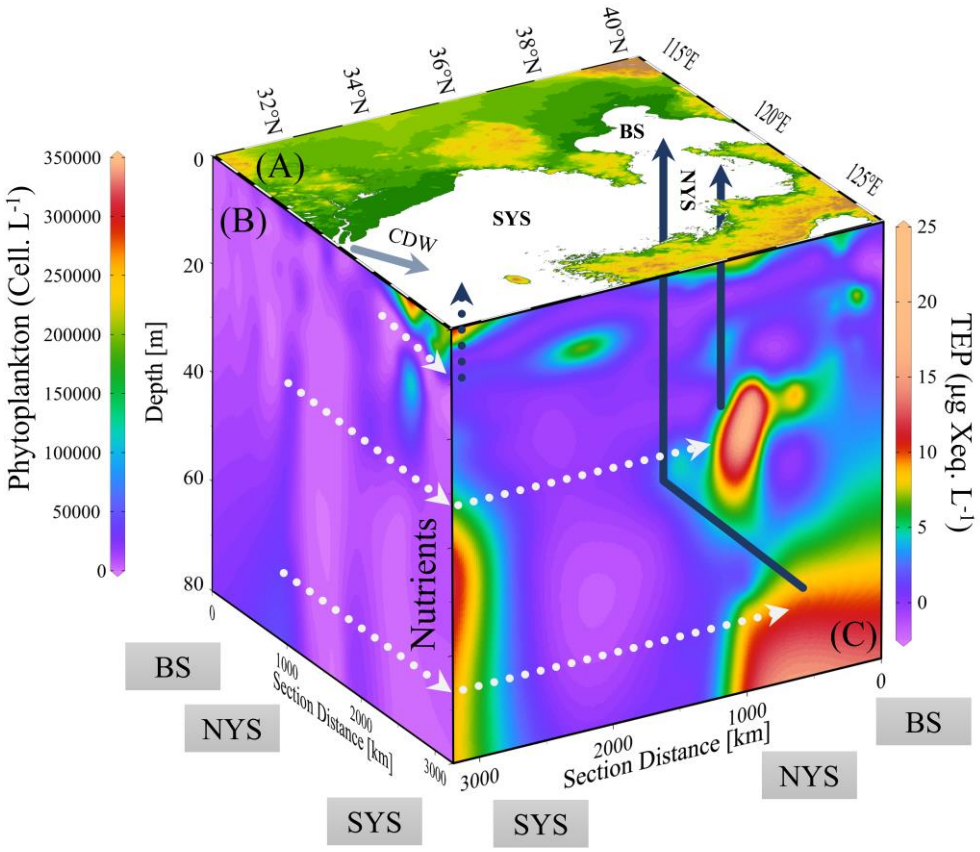

Figure 10. Conceptual model of seasonal average TEP aggregations (C) along study area (A) under the influences of phytoplankton (B)**.** Arrows are projecting the relations (White arrows) and influences of assemblage (Blue arrows) through particular distances of associated seas.